WEST YOST
Water. Engineered.

23692 Birtcher Drive
Lake Forest CA 92630

949.420.3030 phone
530.756.5991 fax
westyost.com

TECHNICAL MEMORANDUM

DATE: September 23, 2022 Project No.: 941-80-21-62

TO: Ground-Level Monitoring Committee (GLMC)
Chino Basin Watermaster

FROM: Eric Chiang, PhD
Lauren Salberg

REVIEWED BY: Andy Malone, PG

SUBJECT: Construction and Calibration of One-Dimensional Compaction Models in the Northwest MZ-1 Area of the Chino Basin

DRAFT

BACKGROUND AND OBJECTIVES

The Chino Basin Watermaster's Subsidence Management Plan (SMP)[1] states that if data from existing monitoring efforts in the Areas of Subsidence Concern indicate the potential for adverse impacts due to subsidence, Watermaster will revise the SMP to avoid those adverse impacts. Watermaster has been monitoring vertical ground motion in Northwest MZ-1 via InSAR since the development of its original SMP (WEI, 2007). Land subsidence in Northwest MZ 1 was first identified as a concern in 2006 in the MZ 1 Summary Report (WEI, 2006). Of particular concern, the subsidence across the San Jose Fault in Northwest MZ 1 has occurred in a pattern of concentrated differential subsidence—the same pattern of differential subsidence that occurred in the Managed Area during the time of ground fissuring. Ground fissuring is the main subsidence related threat to infrastructure.

The issue of differential subsidence, and the potential for ground fissuring in Northwest MZ 1, has been discussed at prior meetings of the Ground Level Monitoring Committee (GLMC), and the subsidence has been documented and described as a concern in Watermaster's State of the Basin Reports, the annual reports of the GLMC, and in the Initial Hydrologic Conceptual Model and Monitoring and Testing Program for the Northwest MZ 1 Area (WEI, 2017). Watermaster increased monitoring efforts in Northwest MZ 1 beginning in Fiscal Year (FY) 2012/13 to include ground elevation surveys and electronic distance measurements (EDM) to monitor ground motion and the potential for fissuring.

In 2015, the Watermaster's Engineer developed the *Work Plan to Develop a Subsidence Management Plan for the Northwest MZ-1 Area* (Work Plan).[2] The Work Plan is characterized as an ongoing

[1] Wildermuth Environmental, Inc. 2015. Chino Basin Subsidence Management Plan. Prepared for the Chino Basin Watermaster. July 23, 2015.

[2] Wildermuth Environmental, Inc. 2015. Work Plan to Develop a Subsidence-Management Plan for Northwest MZ-1. Prepared for the Chino Basin Watermaster. July 23, 2015.

Watermaster effort and includes a description of a multi-year scope of work, a cost estimate, and an implementation schedule. The Work Plan was included in the SMP as Appendix B. Implementation of the Work Plan began in July 2015. On an annual basis, the GLMC analyzes the data and information generated by the implementation of the Work Plan. The results and interpretations generated from the analysis are documented in the annual report of the GLMC and used to prepare recommendations for future activities.

The Work Plan includes various tasks that involve the construction, calibration, and use of one-dimensional aquifer-system compaction models in Northwest MZ-1 (1D Models):

- Tasks 3 and 4 called for the construction and calibration of a single 1D Model at the location of Monte Vista Water District Well 28 (MVWD-28). This 1D Model was used to explore preliminary methods to manage pumping and recharge to avoid the future occurrence of land subsidence in Northwest MZ-1.
- Task 7 called for the construction and calibration of another 1D Model at the location of Pomona Extensometer (PX), which is based on the detailed lithologic information collected at the PX.

The main objective of this technical memorandum is to describe the methods and results for the construction and calibration of both 1D Models. Ancillary objectives are to describe the subsidence mechanisms and the vertical distribution of pre-consolidation head[3] within the aquifer system in Northwest MZ-1.

The knowledge of the subsidence mechanisms and pre-consolidation heads can provide guidance for the Chino Basin parties in the development of "subsidence-management alternatives" (i.e., managed pumping and/or recharge) to avoid the future occurrence of land subsidence in Northwest MZ-1. Subsequent tasks in the Work Plan will utilize the 1D Models described herein to evaluate the effectiveness of the subsidence-management alternatives.

METHODS

This section describes:

- Background information on the modeling tools used to estimate head changes and aquifer system deformation.
- The technical methods that were applied to construct and calibrate the two 1D Models in Northwest MZ-1.

Model Codes Used

The United States Geological Survey (USGS) has developed a wide range of computer models to simulate saturated and unsaturated subsurface flow, solute transport, and chemical reactions in groundwater systems. The most widely used of these models is MODFLOW, which simulates three-dimensional (3D)

[3] The pre-consolidation head is the lowest piezometric level that an aquifer system has ever experienced. When piezometric levels are below the pre-consolidation head, permanent subsidence is caused.

DRAFT

groundwater flow using the finite-difference method. Although it was conceived solely as a groundwater flow model in 1984 and released in 1988 (McDonald et al., 1988), the MODFLOW modular structure has provided a robust framework for the integration of additional simulation capabilities that build on and enhance its original scope. The family of MODFLOW-related models now includes capabilities for simulating coupled groundwater/surface water systems and solute transport.

MODFLOW-NWT (Niswonger et al., 2011) was chosen for this project because: 1) it has extensive publicly available documentation, 2) it has sustained rigorous USGS and academic peer review, 3) it has a long history of development and use, 4) it is widely used around the world in public and private sectors, 5) it can easily operate with additional simulation tools published by others, and 6) it has been used by the Watermaster in the Chino Valley Model (CVM) for the latest Safe Yield Recalculation (WEI, 2020).

The Interbed Storage Package (Leake and others, 1991) of MODFLOW-NWT was chosen to simulate the aquifer-system deformation that is caused by elastic and/or inelastic deformation of the fine-grained interbeds in an aquifer-system due to changes in the effective stress on the soil skeleton because of changing groundwater levels.

How MODFLOW Works

In a MODFLOW model, an aquifer system is represented by a discretized domain consisting of an array of finite difference blocks (model cells) and nodes at the cell centers. The figure below shows the spatial discretization scheme of an aquifer system with a mesh of model cells and nodes at which hydraulic heads are calculated. Hydrostratigraphic units can be represented by one or more model layers and the layer of thickness may vary from cell to cell. The nodal grid forms the framework of a finite-difference numerical model.

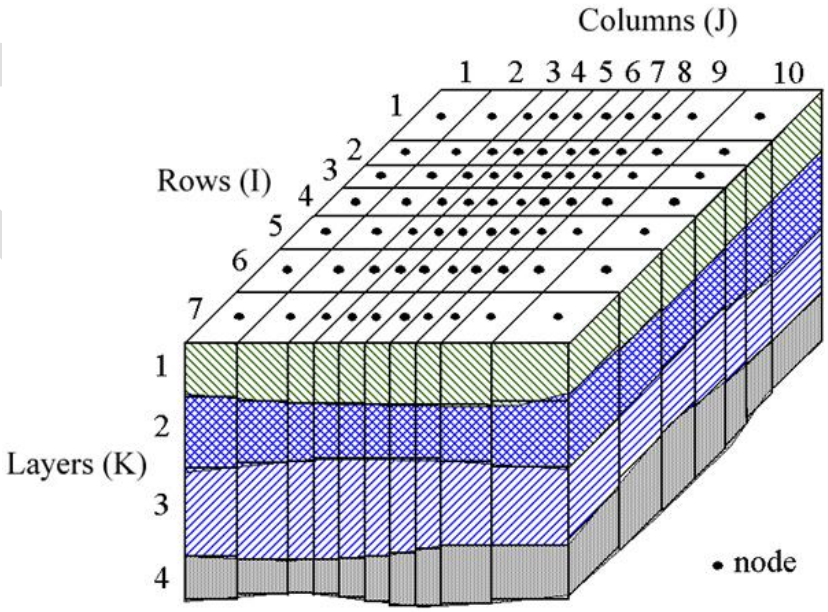

Spatial discretization scheme of MODFLOW

To calculate the hydraulic heads at the nodes (i.e., centers of model cells), a water balance equation is formulated for each model cell:

$$\Sigma Q = S_s \cdot \frac{\Delta h}{\Delta t} \cdot V + S' \cdot \frac{\Delta h}{\Delta t} \quad (1)$$

The left-hand side of the equation (ΣQ) is the sum of all flows to/from neighboring cells, pumping, and recharge occurring within the model cell. The right-hand side represent the storage change within a time-interval of the length Δt, where Ss is the specific storage (that accounts for compressibility of water), S' is the Skeletal storage coefficient (that accounts for compressibility of soil skeleton) of the model cell, V is the volume of the model cell, and Δh is the head change in the model cell over the time interval Δt. The flows to/from neighboring cells can be expressed with the hydraulic heads of the model cell and its neighbors through the Darcy's law that describes the relationship between the flow, hydraulic conductivity, and hydraulic gradient. In summary, equation (1) can be rewritten to an equation containing unknown hydraulic head values at the cell and its neighboring cells with other aquifer property terms.

MODFLOW formulates such an equation for each of the active model cells (where the heads are unknown and need to be solved). Once all equations are formulated, the system of equations are solved together for the unknown head values. Once the head values are computed, they are used to back-calculate the cell-by-cell flow terms. The calculated head values and flow terms are the basis for water budget calculation, particle tracking simulations, transport models, and visualization, such as flow vectors and water level contours.

Estimating the vertical aquifer-system deformation in a model cell

The vertical deformation of a model cell (Δb) over a time interval Δt is calculated as:

$$\Delta b = S' \cdot \Delta h \quad (2)$$

Soil skeleton deformation behavior is non-linear and is dependent on the current hydraulic head and the lowest hydraulic head (i.e., highest effective stress) that has ever been applied to the soil skeleton. To better approximate the non-linear behavior, equation (2) is further refined as follows:

$$\Delta b_e = S_{fe} \cdot \Delta h \qquad if\ h > h_c \quad (3a)$$

$$\Delta b_v = S_{fv} \cdot \Delta h \qquad if\ h \leq h_c \quad (3b)$$

The variable h_c is the pre-consolidation head (also referred to as critical head, or the previous lowest hydraulic head) of the model cell; Δb_e is the elastic deformation; S_{fe} is the elastic storage coefficient; Δb_v is the inelastic deformation; and S_{fv} is the inelastic storage coefficient. Equation (3a) applies when the hydraulic head is greater than the pre-consolidation head. Equation (3b) applies when the hydraulic head is equal or less than the pre-consolidation head.

If the hydraulic head remains greater than the pre-consolidation head, a further decrease in hydraulic head (i.e., increase in effective stress) causes a small elastic compression in both the coarse- and fine-grained sediments. This compression is recoverable if the head returns to its initial value. If the hydraulic head falls below the pre-consolidation head, the fine-grained sediments can compact inelastically. Inelastic compaction is explained by a physical rearrangement of the sediment grains and is largely permanent (Meade, 1964). Inelastic compaction of coarse-grained sediments is generally negligible compared to that of fine-grained sediments. For the same magnitude of changes in effective

stress, inelastic compaction can be one to two orders of magnitude larger than elastic compression (Riley, 1969; Riley 1998).

Time Delay of Compaction

Because of the characteristically low vertical hydraulic conductivity of fine-grained interbeds, the equilibration of hydraulic heads in the interbeds of an aquifer system typically lags the head changes in the bounding aquifers (Hoffmann and others, 2003). In the context of interbed compaction and land subsidence, the time delay caused by slow dissipation of transient overpressures in fine-grained interbed sediments is often given in terms of the time constant τ_0.

$$\tau_0 = \left(\frac{b_0}{2}\right)^2 / D' \quad (4)$$

The time constant τ_0 is the time during which about 93 percent of the ultimate compaction for a given decrease in head occurs (Hoffmann and others, 2003) if the overpressures dissipate vertically in two directions into the bounding aquifers. The variable b_0 is the thickness of the interbed within a model cell and $D' = S_s'/VK_v'$ is the ratio of the specific storage (S_s') and the vertical hydraulic conductivity (VK_v') of the interbed. If the time constant τ_0 is significantly greater than the model time steps, the process of slow dissipation of the heads in the interbed must be explicitly simulated (Hoffmann and others, 2003). For most regional 3D groundwater models with large interbed thickness within model layers (such as CVM), the time constant τ_0 is often much greater than the model time steps. The Subsidence and Aquifer Compaction (SUB) Package introduces an approximation method to simulate the slow dissipation of heads in such models, where all interbeds within a model cell (of greater thickness) are lumped together and their root mean square of the thicknesses is used in the simulation. While this method is theoretically sound, it is impractical to accurately collect details of all interbed data for deep aquifers of a 3D model.

To address this challenge, this work used a combination of 3D and 1D models. In this approach, a 3D model is used to simulate regional groundwater head without the skeleton compression (i.e., compaction) terms. A vertical 1D model at a desired location with detailed lithological log is constructed with much higher vertical resolution, where thickness of each model cell is much smaller than the 3D model to obtain a proper time constant τ_0 for given time step lengths. The simulated heads from the 3D model are then assigned as the prescribed heads for the 1D model cells with coarse-grained sediments, and the 1D model run is executed to calculate the vertical aquifer-system deformation within the model cells of fine-grained sediments. The detailed steps of this approach are given below.

Steps to Construct and Calibrate 1D Compaction Models

In summary, the major steps to construct and calibrate the 1D Models were:

1. Construct the 1D Models using the Interbed Storage Package (Leake and others, 1991) of MODFLOW-NWT at areas of maximum historical subsidence. These models are a vertical stack of cells that represent the aquifer system at each location. The thicknesses of the 1D Model cells are chosen to ensure that the time constant τ_0 is smaller than model time steps. The model cells are categorized into either “Sand” for coarse-grained sediments or “Clay” for fine-grained sediments based on borehole lithologic and geophysical data. Initial aquifer (Sand) and aquitard (Clay) properties were assigned to the 1D Model cells.

DRAFT

2. Prepare a time-series of historical heads by aquifer-system layer to serve as input data for the 1D Models over the calibration period. For 1930-1977, these heads are estimated based on the measured groundwater elevations at wells in the vicinity of the 1D Models. For 1977-2018, these heads are estimated from CVM output data for heads at the 1D Model locations by model layer. The heads are assigned as prescribed heads to the corresponding Sand cells in the 1D Model.

3. Run and calibrate the 1D Models over a historical period by adjusting the aquifer and aquitard properties. The 1D Model simulations were executed to compute a time series of vertical aquifer-system deformation in each 1D Model cell. During calibration, the aquitard properties were adjusted manually to best match historical observations of land subsidence with model-simulated compaction of the aquifer system. The sum of the calculated vertical deformation in all 1D Model cells was assumed to represent the vertical ground motion at the land surface.

RESULTS

This section describes the results and conclusions of the construction and calibration the 1D Models.

Location of the 1D Models

Two 1D Models were constructed and calibrated to simulate the vertical deformation of the aquifer-system sediments at sites in Northwest MZ-1. Figure 1 shows that one model is located at the PX facility and the second model is located at the MVWD-28 well site. Figure 1 also shows the contours of InSAR-estimated vertical ground motion across Northwest MZ-1 used to calibrate the 1D Models and the locations of nearby benchmarks (B-401, B-403, BM 2867, BM 4311, EV3052, EV3054) at which surveyed elevation data are available to validate the 1D Model calibrations.

The PX and MVWD-28 sites were chosen as the 1D Model locations because:

1. Both sites are located within the area of greatest subsidence in Northwest MZ-1 as estimated by InSAR from 1992-2021.

2. The boreholes were drilled to total depths of 1,290 and 1,317 feet below ground surface (ft-bgs) for PX and MVWD-28, respectively. These depths are deeper than most production wells in the area and penetrate all five model layers as currently conceptualized in the CVM.

3. The borehole lithologic descriptions are consistent with the borehole resistivity logs. This is important because the borehole lithology was the primary information used to construct and discretize the 1D Models into “Sand” and “Clay” layers.

Data for Calibration and Validation

Both models were calibrated to match the InSAR estimates of vertical ground motion at the locations of the 1D Models. In addition, ground-level survey data at nearby benchmarks were used to validate the calibration. The table below describes the time range of the available InSAR and ground-level survey

DRAFT

data, including data provided by the Los Angeles Department of Public Works (LADPW)[4] and the data acquired by the Chino Basin Watermaster as part of its Ground-Level Monitoring Program.

Time Range of Ground-Motion Data Used in 1D Model Calibration and Validation	
Location/Method	Time Range
InSAR at the PX and MVWD-28 locations	1992 to 1999, and 2005 to 2020
Benchmark 2867 via LADPW leveling surveys	1990 to 2013
Benchmark 4311 via LADPW leveling surveys	1990 to 2013
Benchmarks B-401 and B-403 via CBWM leveling surveys	2013 to 2021

Borehole Lithology

The lithology at PX and MVWD-28 consists of coarse-grained "Sand" layers comprised of silty sands, sands, and gravels, interbedded with fine-grained "Clay" layers comprised of silts, silty clays, and clays.[5] The table below shows the mapping of Unified Soils Classification System (USCS) codes to "Sand" or "Clay" layers.

Mapping of USCS Codes to Sand or Clay Layers		
USCS Code	Cell Type	Description
SP-SM	Sand	Poorly graded sand with silt
SP-SC	Sand	Poorly graded sand with clay
SP	Sand	Poorly graded sand with gravel
SC	Sand	Clayey sand or Sand with clay
SM	Sand	Silty sand
CH	Clay	Fat clay
ML	Clay	Sandy silt
CL	Clay	Sandy lean clay or Clay with sand

Spatial Discretization

Figures 2 and 3 show the generalized borehole lithology at the PX and MVWD-28 sites, short-normal borehole resistivity logs, 1D Model cells (Sand cells are shaded in blue; Clay cells are shaded white), and the corresponding CVM layers. CVM Layer 1 represents the shallow aquifer-system and is generally characterized by unconfined to semi-confined groundwater conditions. CVM Layers 2 to 5 represent the deep aquifer-system and are characterized by confined groundwater conditions, lower permeability

[4] https://dpw.lacounty.gov/sur/BenchMark/

[5] The PX2 and MVWD-28 borehole lithologic and geophysical logs are included in Attachment A to this memorandum.

sand and gravel layers (compared to Layer 1), and a greater abundance of interbedded fine-grained sediments.

For the PX 1D Model, the borehole lithology was discretized into a stacked column of 529 two-foot-thick cells starting from 234 ft-bgs to 1,292 ft-bgs. The uppermost 234 feet of sediments were not included in the 1D Model because the sediment was unsaturated throughout the simulation and therefore not subject to deformation caused by changes in head. Each 1D Model cell was mapped to the borehole lithology and identified as either a "Sand" or "Clay" cell based on the mapping shown in the table above.

For the MVWD-28 1D Model, the borehole lithology was discretized into a stacked column of 510 two-foot-thick cells starting from 280 ft-bgs to 1,300 ft-bgs. The uppermost 280 feet of sediments were not included in the 1D Model because the sediment was unsaturated throughout the simulation and therefore not subject to deformation caused by changes in head. Each model cell was mapped to the borehole lithology and identified as either a "Sand" or "Clay" cell based on the mapping shown in the table above.

Time Discretization

The 1D Models were ran from July 1, 1930 to June 30, 2018 on a monthly time step.

Initial Conditions

The 1D Models require assignment of initial conditions for head, pre-consolidation head, and initial compaction for each model cell. An initial head of 750.5 feet above sea level (ft-amsl) was assigned to all model cells based on measured heads in 1930 at wells located in the vicinity of the 1D Models. The assumption here is that 1930 was a time before significant head declines and compaction of the aquifer-system sediments in Northwest MZ-1. The initial pre-consolidation head was also set at 750.5 ft-amsl. The initial compaction was set to zero for all model cells.

Boundary Conditions

The Sand cells in the 1D Models were modeled as a specified-head boundary with the Flow and Head Boundary Package (Leake and others, 1997). Figures 4 and 5 show the time-series of groundwater elevations by CVM Layer that were used in the 1D Models for the PX and MVWD-28 sites, respectively. Historical measured heads at several wells located in the vicinity of the 1D Models are also shown on Figures 4 and 5.

For the period 1930-1977, the measured heads at nearby wells were used to estimate the time-series of groundwater elevations by CVM Layer. Figure 6 shows that during this period, virtually all pumping wells that existed in Northwest MZ-1 had well screens that penetrated Layer 1 only. Figures 4 and 5 show that during 1930-1977 it was assumed that heads in the deeper CVM Layers equilibrated simultaneously with the head declines that were occurring in Layer 1.

For the period 1977-2018, the CVM-simulated heads at the 1D Model locations were used as the time-series of groundwater elevations by CVM Layer. This period is the calibration period for the 2020 CVM. Figure 6 shows that during this period, deeper pumping wells were constructed in Northwest MZ-1. Figures 4 and 5 show that after about 1977, the deeper pumping caused head declines in the deeper confined CVM Layers, which in turn resulted in upward vertical hydraulic gradients.

DRAFT

Initial Aquifer/Aquitard Properties

Table 1 lists the initial estimates for vertical hydraulic conductivity, specific storage, and the inelastic and elastic storage coefficients that were assigned to all Sand and Clay cells in both 1D Models. These initial estimates were obtained based on literature reviews and were adjusted during calibration.

Calibration of the 1D Models

The calibration of the 1D Models was performed in a manual and iterative manner in the following steps:

1. The initial estimates of parameter values for the Sand and Clay cells were assigned to the 1D Models.
2. The 1D Models were executed from 1930 to 2018 using the prescribed heads by model layer in Figures 4 and 5 as boundary conditions for the Sand cells in the 1D Models.
3. The model-simulated compaction values in the combined Clay cells were compared with the InSAR estimates of vertical ground motion over the period of InSAR records, and the goodness of fit was determined via visual and statistical methods.
4. A new set of parameter values for the Clay[6] cells were determined based on the results of step 3, and steps 1 to 3 were repeated for a new calibration iteration.

The iterative calibration process described above was repeated until a good match between model-simulated aquifer-system deformation and the InSAR estimates of vertical ground motion was achieved with parameter values within reasonable bounds. The initial parameter values in Table 1 were used in calibration iteration v1, and then manually adjusted in subsequent calibration iterations.

Table 2 is a list of calibration iterations (v1 to v21) and parameter values for the Clay cells in both 1D Models. Figures 7 and 8 show the time series of the simulated aquifer-system deformation and observed vertical ground motion for all calibration iterations for the PX 1D Model and the MVWD-28 1D Model, respectively. The time-series of vertical ground motion from the benchmark surveys are also displayed on these figures to validate the calibration results. The calibration process was focused on matching model results with the recent InSAR data (i.e., 2005 to 2020), since these are considered the most reliable InSAR data for calibration targets.

For the PX 1D Model, the parameters values for calibration iterations V13 and V21 provided the best match between the simulated and observed values. For the MVWD-28 1D Model, the parameter values for calibration iterations V7 and V21 provided the best match between the simulated and observed values. For both models, V21 matches the InSAR data from 1992 to 1999 better. V21 also results in less total subsidence compared to V7 and V13, which is more consistent with no reported observations of ground fissuring or subsidence-related impacts to overlying infrastructure.

The final calibration results for v21 are displayed in the following figures and tables for both 1D Models:

[6] The potential for compaction in the Sand cells was assumed to be negligible, hence, the parameter values for the Sand cells were set to their initial values in Table 1 and were not adjusted during 1D Model calibration.

DRAFT

- Figures 9 and 10 are time series charts that compare simulated versus observed data for calibration iteration v21 for the PX 1D Model and the MVWD-28 1D Model, respectively.
- Figures 11 and 12 are scatter plots that compare simulated versus observed data, which quantifies the goodness of fit of the calibration iterations. On these charts, the X-axis represents measured ground motion and the Y-axis represents the model-simulated aquifer-system deformation. The orange diagonal line represents the line of perfect fit.
- Tables 3 and 4 shows the calibration statistics for all calibration iterations, which indicate that v21 is the best calibration for both 1D Models.

Figures 9 and 10 also display the ground-level survey data from 1990-2020 that validate the model calibration for v21. There are no ground-level survey data near the PX and MVWD-28 sites prior to the 1990s that can be used to validate v21. However, Figure 1 shows that 3.5 feet of subsidence occurred at benchmark EV3052 from 1923-1974 and 1.64 feet of subsidence occurred at benchmark EV3054 from 1968-1978. These early ground-level survey data are consistent with the timing and magnitude of the compaction that was estimated by the 1D Models prior to the 1990s.

In conclusion, the 1D Model parameters of v21 resulted in the best fit between simulated compaction and the observed subsidence data. The final calibrated parameters for both 1D Models are listed below:

Final Calibrated Parameter Values for the Clay Cells in the PX and MVWD-28 1D Models

Iteration	VK [ft/day]	Ss [1/ft]	Sfv [-]	Sfe [-]
V21	2.00E-07	1.14E-05	4.50E-04	4.50E-06

Simulation of Historical Subsidence

Figure 7 shows that the final calibration run (V21) for the PX 1D Model resulted in a total of about 9.6 feet of aquifer-system compaction from 1930 to 2018. Most of the compaction (about 6.4 feet) occurred between 1930 and 1978—the period of gradual and persistent lowering of groundwater levels by about 190 feet in Northwest MZ-1.

Figure 8 shows that the final calibration run (V21) for the MVWD-28 1D Model resulted in a total of about 5.5 feet of aquifer-system compaction from 1930 to 2018. About three feet of compaction occurred between 1930 and 1978—the period of gradual and persistent lowering of groundwater levels by about 190 feet in Northwest MZ-1.

The final calibration run (v21) also generated end-of-calibration (2018) estimates of the compaction and critical head in the 1D Model cells, which are displayed on Figures 13 and 14 for the PX and MVWD-28 1D Models, respectively. The higher critical head and lower compaction in the center of thicker fine-grained sediment layers indicate that the pore pressures there have not yet dissipated and, therefore, these sediment layers are susceptible to compaction should the internal pore pressures continue to decline in the future. As thicker fine-grained layers are primarily located in the deep aquifer-system, this indicates that the potential for future compaction is more likely to occur in the deep aquifer system (Layers 2, 3, 4, and 5) compared to the shallow aquifer-system (Layer 1).

DRAFT

Sensitivity Analysis

In early 2022, the GLMC reviewed the calibration results of the 1D Models described above and recommended an analysis to evaluate the sensitivity of the 1D Model calibrations to the estimates of historical heads. This sensitivity analysis is prudent given the lack of historical data, and hence, uncertainty in knowledge of depth-specific historical heads (i.e., the time series of historical heads in each model layer).

The sensitivity analysis was performed using the following methods:

1. Adjust the time series of historical heads shown in Figures 4 and 5 to prepare six additional calibration runs—three for the PX 1D Model and three for the MVWD-28 1D Model:

    i. **Calibration Run V22 for the PX 1D Model**. Figure 15 displays a time series of historical heads at the PX site where declines in heads in Layer 5 lag behind the declines in heads in Layers 1 and 3 over the period of 1930-1977. This time series is plausible since there are no records of pumping wells in Northwest MZ-1 with well screens that penetrate Layer 5 during 1930-1973 (see Figure 6).

    ii. **Calibration Run V23 for the PX 1D Model**. Figure 16 displays a time series of historical heads at the PX site where: (i) heads in Layer 1 were adjusted upward from 1978-2018 to better match recent heads measured at the PX1-1 piezometer (Layer 1) in 2020 and (ii) heads in Layer 5 were adjusted downward from 1978-2018 to better match recent heads measured at the PX2-3 piezometer (Layer 5) in 2020.

    iii. **Calibration Run V24 for the PX 1D Model**. Figure 17 displays a time series of historical heads at the PX site where heads were adjusted as described in V22 and V23.

    iv. **Calibration Run V22 for the MVWD-28 1D Model**. Figure 18 displays a time series of historical heads at the MVWD-28 site where declines in heads in Layer 5 lag behind the declines in heads in Layers 1 and 3 over the period of 1930-1977. This time series is plausible since there are no records of pumping wells in Northwest MZ-1 with well screens that penetrate Layer 5 during 1930-1973.

    v. **Calibration Run V23 for the MVWD-28 1D Model**. Figure 19 displays a time series of historical heads at the MVWD-28 site where: (i) heads in Layer 1 were adjusted upward from 1978-2018 to better match recent heads measured at the PX1-1 piezometer (Layer 1) in 2020 and (ii) heads in Layer 5 were adjusted downward from 1978-2018 to better match recent heads measured at the PX2-3 piezometer (Layer 5) in 2020.

    vi. **Calibration Run V24 for the MVWD-28 1D Model**. Figure 20 displays a time series of historical heads at the MVWD-28 site where heads were adjusted as described in v22 and V23.

2. The 1D Models were executed from 1930 to 2018 using the prescribed heads by model layer in V22, V23, and V24 as boundary conditions for the Sand cells in the 1D Models.

3. The model-simulated compaction values in the combined Clay cells were compared with the InSAR estimates of vertical ground motion over the period of InSAR records, and the goodness of fit was determined:

- Figures 21, 22, and 23 are time series charts that compare simulated versus observed data for calibration iterations V22, V23, and V24 for the PX 1D Model.
- Figures 24, 25, and 26 are time series charts that compare simulated versus observed data for calibration iterations V22, V23, and V24 for the MWWD-28 1D Model.
- Tables 3 and 4 shows the calibration statistics for calibration iterations V22, V23, and V24 for PX 1D Model and the MWWD-28 1D Model, respectively.

The main observations and conclusions from the sensitivity analysis are:

- The adjustment in historical heads in the sensitivity analysis did not significantly affect the simulated compaction in the 1D Models. This observation indicates that the 1D Models are not sensitive to minor differences in the assumptions for historical heads. More likely, the 1D Models are most sensitive to the number and thicknesses of the Clay layers and the long-term declining trends in historical heads that drive the delayed drainage and compaction of the Clay layers.
- The 1D Model calibrations with V24 were virtually identical to V21 with no changes to the parameter values for the Clay cells as determined in V21.
- V24 also resulted in less total compaction compared to V21 in both 1D Models, which is more consistent with no reported observations of ground fissuring or subsidence related impacts to overlying infrastructure. Therefore, V24 replaces V21 as the final calibration iteration, but with no changes to the model parameters determined in V21.
- The 1D Models are well calibrated and capable of accurately estimating future aquifer-system compaction under various plans for pumping and recharge. Therefore, the GLMC should proceed with the use of the 1D Models to develop subsidence management strategies for Northwest MZ-1, if necessary.

MODEL ERRORS AND LIMITATIONS

In general, a groundwater model is a simplified mathematical representation of a complex hydrogeologic system. Because of this, there are limits to the accuracy of the model and the use and interpretation of the model results. There are various sources of error and uncertainty. Model error commonly stems from the conceptual model, practical limitations of grid cell size and time discretization, parameter structure, insufficient calibration data, and the effects of processes not simulated by the model. These factors, along with error in observations, result in uncertainty in model results.

The potential errors and limitations associated with the 1D Models and their calibration include:

- The 1D Models were based on the limited resolution, depth, and accuracy of the description of the aquifer-system sediments as documented on the driller's logs of PX and MVWD-28 boreholes.
    - The resolution by depth interval of the lithologic descriptions in this log are typically greater than five feet, which may not be a fine enough resolution to characterize any

thinner interbedding of aquifer and aquitard layers that are an important control on aquifer-system deformation.

- The boreholes did not penetrate the full thickness of the semi-consolidated bedrock formations; there may be deforming sediments at depths below the borehole bottom that are responsible for some of the vertical ground motion estimated by InSAR.

- Most wells in Northwest MZ-1 have well screens that only penetrate the shallow aquifer-system or penetrate both the shallow and deep aquifer-systems. There are no wells in Northwest MZ-1 that existed during the calibration period that are screened only across the deep aquifer-system, meaning that there are no historical measured water-level data for only the deep aquifer-system. As such, there is some uncertainty in the long-term time-series of heads for Layers 2 and 3 that were used as the boundary conditions for the 1D Model calibration, which adds uncertainty to the model results.

- Water-level data at wells is scarce in Northwest MZ-1 prior to the 1930s. This 1D modeling effort assumes that the significant lowering of heads in Northwest MZ-1 began after 1930, which may not be an accurate assumption. If head declines began before 1930, then this could impact the calibration of the 1D models and add uncertainty to the model results.

- The 1D models used InSAR-derived estimates of vertical ground motion as calibration targets for aquifer-system compaction. The limitations of using InSAR-derived estimates as calibration targets are: (1) the InSAR record begins in 1992, which limits the length of the calibration period; (2) there are multiple data gaps in the InSAR record because of satellite malfunctions and satellite replacement; and (3) InSAR produces an aggregate estimate of aquifer-system deformation and therefore provides no depth-specific calibration targets. Due to the lack of depth-specific calibration there is greater uncertainty in the depth-specific estimates for the aquifer and aquitard properties, and hence, the model results.

Continued monitoring and enhanced understanding of hydrogeologic conditions is crucial to minimizing model error and uncertainty, especially the monitoring of the PX in Northwest MZ-1. Future monitoring and data analysis can identify local anomalies associated with geologic complexity that are not currently represented in the model. Model error and uncertainty can be reduced by incorporating new monitoring information into future model updates, if recommended by the GLMC.

NEXT STEPS

Figure 15 is a schedule of activities for the *Development of a Subsidence Management Plan for the Northwest MZ-1 Area* for FY 2021/22. The next steps are as follows:

1. Members of the GLMC are asked to review this draft technical memorandum and provide comments and suggestions to Andy Malone (amalone@westyost.com) and Edgar Tellez-Foster (etellezfoster@cbwm.org) by October 21, 2022. Specifically, Watermaster staff and Engineer ask that the GLMC members answer the following question in their comments: Are the 1D Models as described in this technical memorandum sufficiently calibrated for to estimate the potential for future subsidence under the Baseline Management Alternative (BMA)? The BMA is a planning scenario that represents the Parties' current plans for pumping and recharge in the Chino Basin.

2. The 1D Models are intended to be used to characterize the mechanical response of the aquifer-system to the BMA. A draft technical memorandum will be prepared that summarizes the evaluation of the BMA, particularly, the ability of the BMA to manage piezometric levels in Northwest MZ-1 so that future subsidence is minimized or abated. The draft technical memorandum may also include a recommendation for the Initial Subsidence Management Alternative (ISMA) if the BMA is not successful at managing future subsidence. The assumptions of the ISMA, including the groundwater production and replenishment plans of the Chino Basin parties, will be described in the technical memorandum, and must be agreed upon by the GLMC. A GLMC meeting will be held to review the technical memorandum and the recommended ISMA.
3. After the recommended ISMA is agreed upon by the GLMC, the Watermaster's MODFLOW model will be updated to run the ISMA and will be used to estimate the hydraulic head response to the ISMA at the MVWD-28 and PX locations. The projected hydraulic heads generated from the MODFLOW model using the ISMA will be extracted from the MODFLOW model results at the MVWD-28 and PX locations and will be used as input files for both 1D Models. The 1D Models will then be run to characterize the mechanical response of the aquifer-system to the ISMA at both the MVWD-28 and PX locations to evaluate the effectiveness of the ISMA at managing future subsidence.
4. A draft technical memorandum will be prepared that summarizes the evaluation of the ISMA, particularly, the ability of the ISMA to manage hydraulic heads in Northwest MZ-1 so that future subsidence is minimized or abated. The draft technical memorandum may also include a recommendation for a second Subsidence-Management Alternative (SMA-2), if the ISMA is not successful at managing future subsidence. The assumptions of the SMA-2, including the groundwater production and replenishment plans of the Chino Basin parties, will be described, and must be agreed upon by the GLMC. A GLMC meeting will be held to review the technical memorandum and the recommended SMA-2.
5. If necessary and recommended by the GLMC, additional subsidence management alternative scenarios may be run in FY 2022/23. It is currently envisioned that, based on the results of the 1D Model results, the GLMC may recommend an update to the Watermaster's Subsidence Management Plan in FY 2022/23 to minimize or abate the future occurrence of land subsidence in Northwest MZ-1.

DRAFT

REFERENCES

Hoffmann, J., Leake, S.A.; Galloway, D.L.; Wilson, M.A. (2003). *MODFLOW-2000 Ground-water model--user guide to the Subsidence and Aquifer-System Compaction (SUB) Package*. Open File Report 03-233. - Tucson, AZ : U.S. Geological Survey, 2003.

Leake S. A. and Prudic D. E. (1991) *Documentation of a computer program to simulate aquifer-system compaction using the modular finite-difference ground-water flow model.* Techniques of Water-Resources Investigations 06-A2. - [s.l.] : U. S. Geological Survey, 1991.

Leake S. A. and Lilly M. R. (1997) *Documentation of a Computer Program (FHB1) for Assignment of Transient Specified-Flow and Specified-Head Boundaries in Applications of the Modular Finite-Difference Ground-Water Flow Model (MODFLOW).* Open-File Report 97-571. - Tucson, Arizona : U. S. Geological Survey, 1997.

Meade, R.H., 1964, *Removal of water and rearrangement of particles during the compaction of clayey sediments—review*: U.S. Geological Survey Professional Paper 497-B, 23 p.

Niswonger, R. G., Panday, S., & Ibaraki, M. (2011). *MODFLOW-NWT, A Newton formulation for MODFLOW-2005: U.S. Geological Survey Techniques and Methods 6-A37, 44 p.* Reston, Virginia: U.S. Geological Survey.

Riley, F.S. (1969). *Analysis of borehole extensometer data from central California*: International Association of Scientific Hydrology Publication 89, p. 423–431.

———(1998). *Mechanics of aquifer systems—The scientific legacy of Dr. Joseph F. Poland, in Borchers, J.W., ed., Land subsidence case studies and current research*: Proceedings of the Dr. Joseph F. Poland Symposium on Land Subsidence, Association of Engineering Geologists Special Publication no. 8, p. 13–27.

Wildermuth Environmental Inc. (2017). *Technical Memorandum. Task 3 and Task 4 of the Work Plan to Develop a Subsidence Management Plan for the Northwest MZ-1 Area: Development and Evaluation of Baseline and Initial Subsidence-Management Alternatives.*

Wildermuth Environmental Inc. (2020). *2020 Safe Yield Recalculation Final Report. Prepared for Chino Basin Watermaster.*

DRAFT

Table 1. Initial Estimates of Model Parameters		
Cell Type	Model Parameter	Parameter Value
Sand	Vertical hydraulic conductivity VK	5.00E-01 [ft/day]
Sand	Specific storage Ss	1.83E-06 [1/ft]
Sand	Inelastic storage coefficient Sfv	1.00E-06 [-]
Sand	Elastic storage coefficient Sfe	1.00E-06 [-]
Clay	Vertical hydraulic conductivity VK	2.50E-05 [ft/day]
Clay	Specific storage Ss	1.14E-05 [1/ft]
Clay	Inelastic storage coefficient Sfv	1.65E-04[-]
Clay	Elastic storage coefficient Sfe	4.50E-06 [-]

Table 2. Parameter Values for Clay Cells by Calibration Iteration				
Iteration	VK [ft/day]	Ss [1/ft]	Sfv [-]	Sfe [-]
V1	2.00E-05	1.14E-05	1.65E-04	4.50E-06
V2	1.00E-05	1.14E-05	1.65E-04	4.50E-06
V3	1.00E-06	1.14E-05	1.65E-04	4.50E-06
V3a	1.00E-06	5.00E-06	1.65E-04	4.50E-06
V3b	1.00E-06	7.00E-06	1.65E-04	4.50E-06
V4	2.00E-05	1.14E-05	1.00E-04	4.50E-06
V5	2.00E-05	1.14E-05	2.00E-04	4.50E-06
V6	1.00E-06	1.14E-05	2.00E-04	4.50E-06
V7	1.00E-06	1.14E-05	3.00E-04	8.00E-06
V8	1.00E-06	1.14E-05	5.00E-04	8.00E-06
V9	1.00E-06	1.14E-05	4.50E-04	4.50E-06
V10	5.00E-06	1.14E-05	4.50E-04	8.00E-06
V11	5.00E-06	5.00E-05	4.50E-04	8.00E-06
V12	2.00E-06	1.14E-05	4.50E-04	4.50E-06
V13	1.00E-06	1.14E-05	4.00E-04	4.50E-06
V14	1.00E-06	7.00E-06	4.00E-04	4.50E-06
V15	6.00E-07	1.14E-05	4.50E-04	4.50E-06
V16	8.00E-07	1.14E-05	4.50E-04	4.50E-06
V17	1.00E-06	1.14E-05	3.50E-04	8.00E-06
V18	1.00E-06	1.14E-05	4.00E-04	2.00E-06
V19	4.00E-05	1.14E-05	1.00E-04	4.50E-06
V20	1.00E-06	1.14E-05	3.50E-04	4.50E-06
V21	2.00E-07	1.14E-05	4.50E-04	4.50E-06

Table 3. Calibration Statistics for the PX 1D Model

Iteration	Total Subsidence (ft)	Mean of Differences (Observed - Modeled) (ft)	Standard Deviation (ft)	Root Mean Square Deviation (ft)	R^2	NSE
V1	9.99	0.29	0.35	0.45	0.91	0.47
V2	9.39	0.32	0.35	0.47	0.94	0.45
V3	6.56	0.37	0.31	0.48	0.96	0.27
V4	6.65	0.37	0.31	0.48	0.93	0.28
V5	6.62	0.37	0.31	0.48	0.97	0.28
V3a	6.19	0.29	0.30	0.41	0.86	0.09
V3b	11.97	0.29	0.38	0.48	0.91	0.57
V6	7.69	0.38	0.33	0.50	0.97	0.37
V7	10.69	0.40	0.39	0.56	0.97	0.55
V8	16.04	0.46	0.52	0.70	0.96	0.67
V9	14.78	0.45	0.49	0.66	0.97	0.65
V10	20.39	0.41	0.59	0.72	0.96	0.71
V11	19.83	0.42	0.58	0.71	0.96	0.71
V12	17.13	0.43	0.53	0.68	0.96	0.68
V13	13.47	0.43	0.46	0.63	0.97	0.62
V14	13.54	0.43	0.46	0.63	0.97	0.63
V15	13.08	0.46	0.47	0.66	0.97	0.62
V16	14.04	0.46	0.48	0.66	0.97	0.64
V17	12.11	0.41	0.42	0.59	0.97	0.60
V18	13.48	0.43	0.46	0.63	0.97	0.62
V19	6.34	0.28	0.30	0.41	0.67	-0.08
V21	9.64	0.03	0.08	0.09	0.99	0.98
V22	9.54	0.03	0.08	0.09	0.99	0.98
V23	9.57	0.05	0.09	0.10	0.99	0.97
V24	9.46	0.04	0.09	0.10	0.99	0.97

Table 4. Calibration Statistics for the MVWD-28 1D Model						
Iteration	Total Subsidence (ft)	Mean of Differences (Observed - Modeled) (ft)	Standard Deviation (ft)	Root Mean Square Deviation (ft)	R^2	NSE
V1	6.60	0.23	0.22	0.31	0.83	0.46
V2	6.41	0.21	0.20	0.30	0.85	0.49
V3	4.94	0.12	0.13	0.18	0.96	0.82
V4	4.03	0.27	0.23	0.36	0.72	-0.03
V5	7.96	0.20	0.21	0.29	0.87	0.62
V3a	5.02	0.12	0.13	0.18	0.95	0.82
V3b	4.99	0.12	0.13	0.18	0.95	0.82
V6	5.75	0.07	0.11	0.13	0.97	0.92
V7	7.78	-0.05	0.05	0.07	0.99	0.98
V8	11.09	-0.25	0.11	0.27	0.99	0.85
V9	10.33	-0.21	0.09	0.22	0.99	0.89
V10	15.34	-0.20	0.09	0.21	0.99	0.93
V11	14.98	-0.21	0.09	0.23	0.99	0.92
V12	12.75	-0.25	0.10	0.27	0.99	0.88
V13	9.53	-0.16	0.06	0.17	0.99	0.93
V14	9.60	-0.16	0.06	0.17	0.99	0.93
V15	8.59	-0.14	0.06	0.15	0.99	0.93
V16	9.56	-0.18	0.08	0.20	0.99	0.91
V17	8.68	-0.10	0.05	0.11	0.99	0.97
V18	9.54	-0.16	0.06	0.17	0.99	0.93
V19	4.09	0.28	0.24	0.36	0.72	-0.01
V21	5.53	0.00	0.05	0.05	0.99	0.99
V22	5.41	-0.01	0.05	0.05	0.99	0.99
V23	5.59	-0.01	0.05	0.05	0.99	0.99
V24	5.48	-0.02	0.05	0.05	0.99	0.99

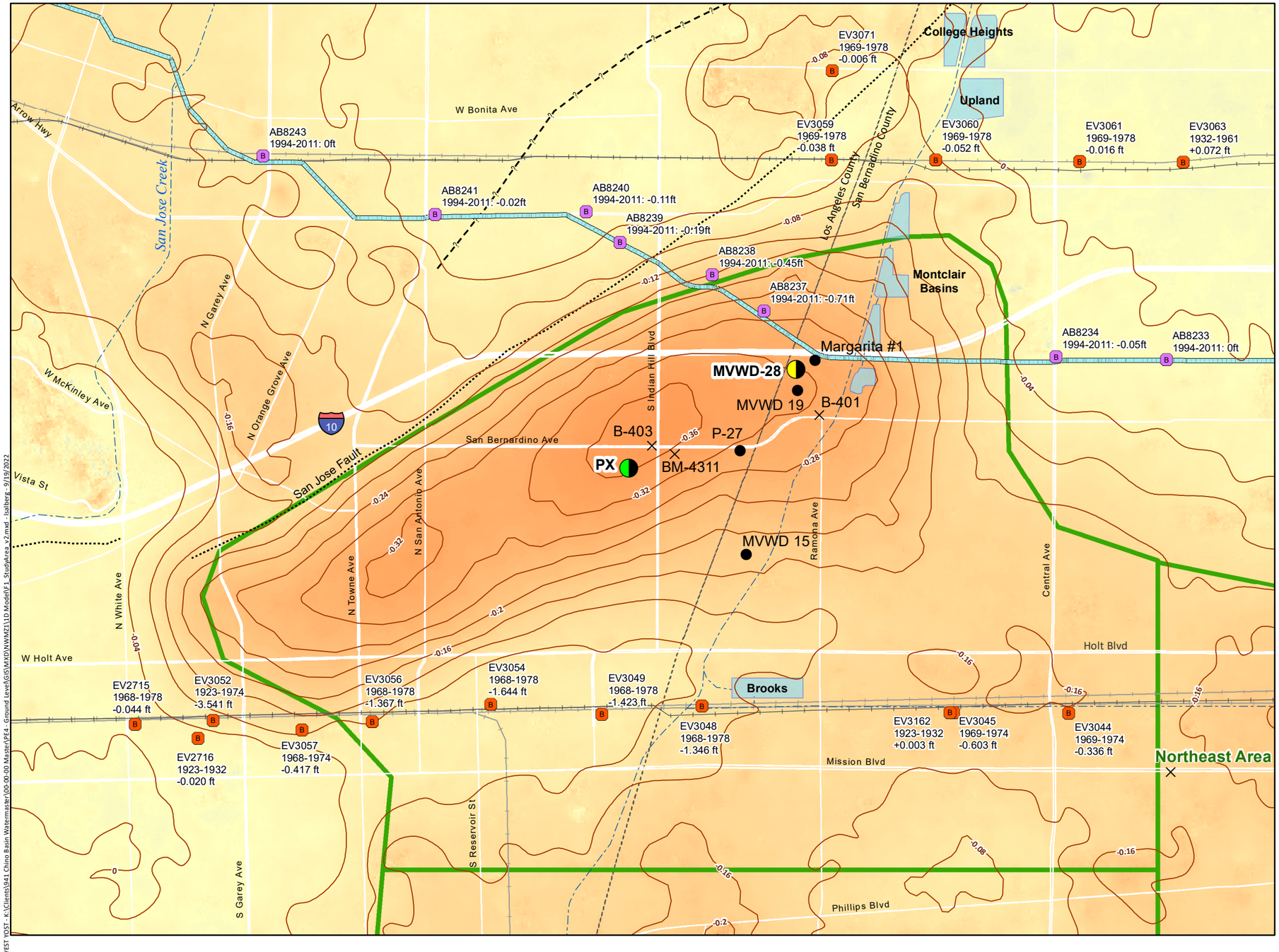

1D Model Locations

- MVWD-28
- PX

Land Subsidence Features

+0.55 ft
0 ft
-0.55 ft

Relative Change in Land Surface Elevation as Estimated by InSAR *(March 2011 to March 2022)*

-1:0- Contours of Relative Change in Land Surface Elevation as Estimated by InSAR *(March 2011 to March 2022)*

- Benchmark used for 1D Model Calibration
- NGS Benchmarks
- MWD Benchmarks

Other Features

- Well with Historical Measured Heads
- Recharge Basin
- Northwest MZ-1 Area of Subsidence Concern
- Fault (dotted where concealed; queried where uncertain)
- MWD Upper Feeder
- Railroads

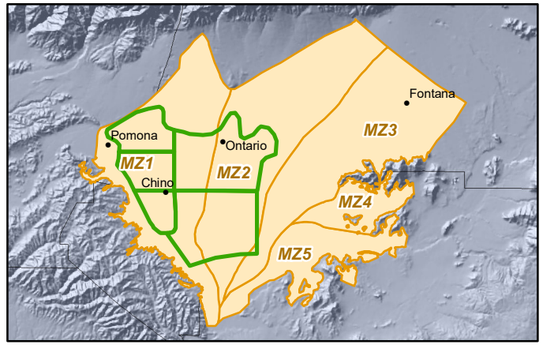

Prepared by:

WEST YOST
Water. Engineered.

N

0 1 2 Miles

0 2 4 Km

Figure 1

Locations of PX and MVWD-28 1D Models and Historical Elevation Surveys at Benchmarks

Chino Basin Watermaster
Ground-Level Monitoring Committee
1D Compaction Models in the Northwest MZ-1 Area

WEST YOST - K:\Clients\941 Chino Basin Watermaster\00-00-00 Master\PE4 - Ground Level\GIS\MXD\WMZ1\1D Model\F1_StudyArea_v2.mxd - lsalberg - 9/19/2022

Figure 2. PX Site: CVM Layers, Borehole Lithology, 1D Model Cells, and Resistivity Log

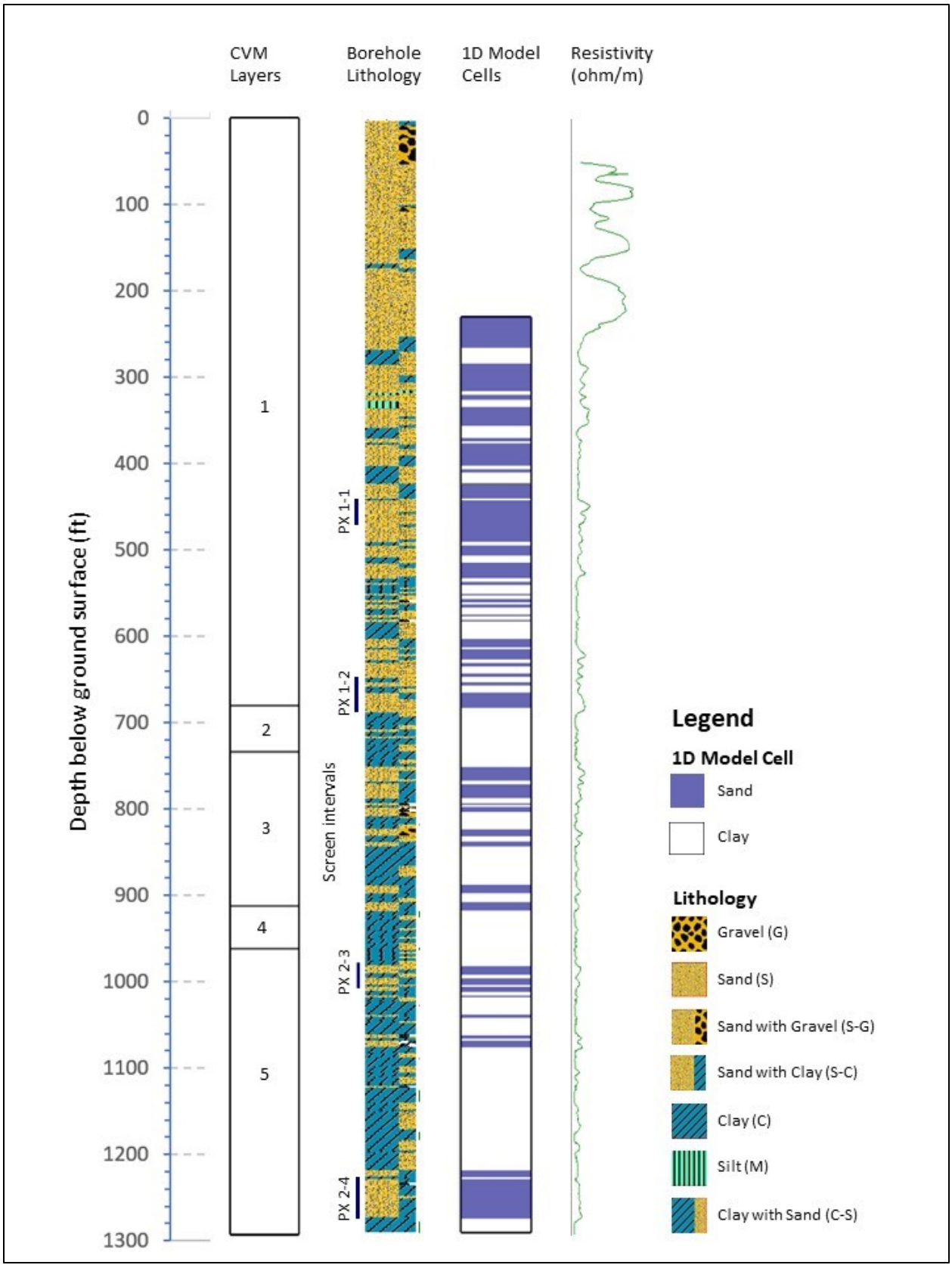

Figure 3. MVWD-28 Site: CVM Layers, Borehole Lithology, 1D Model Cells, and Resistivity Log

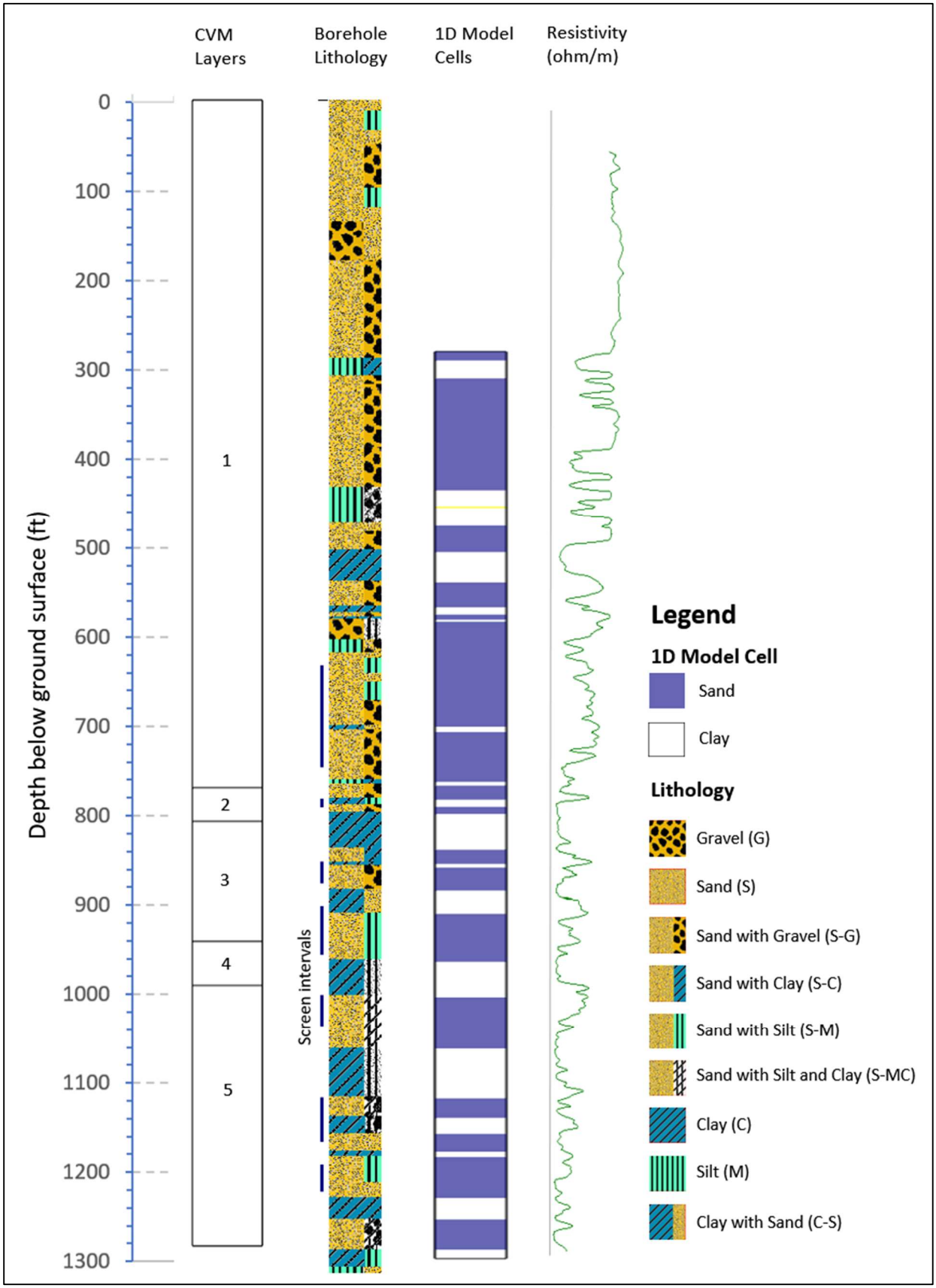

Figure 4. Measured Heads vs. Heads Used in Calibration of PX 1D Model - Calibration Run V21

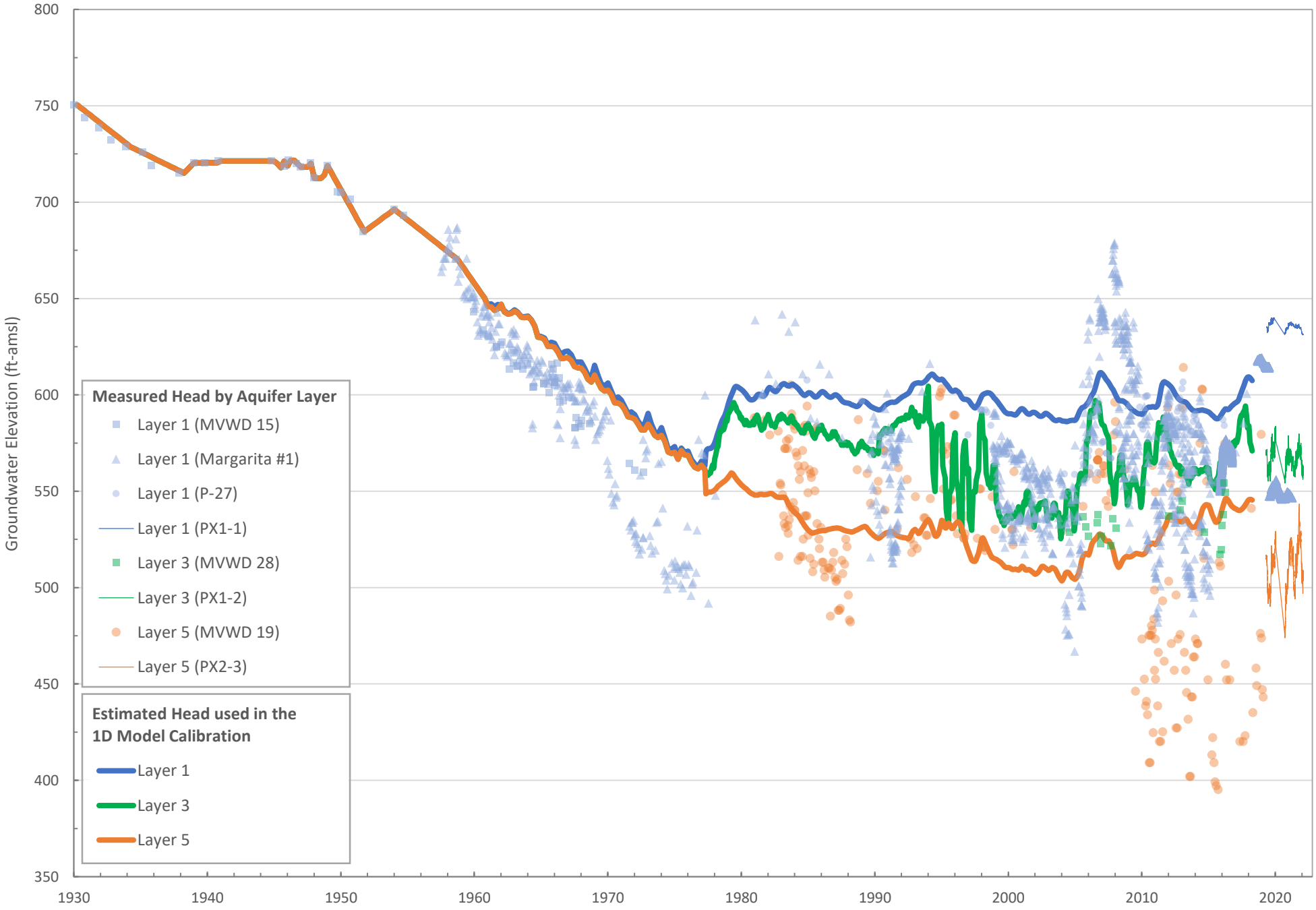

Figure 5. Measured Heads vs. Heads Used in Calibration of MVWD-28 1D Model - Calibration Run V21

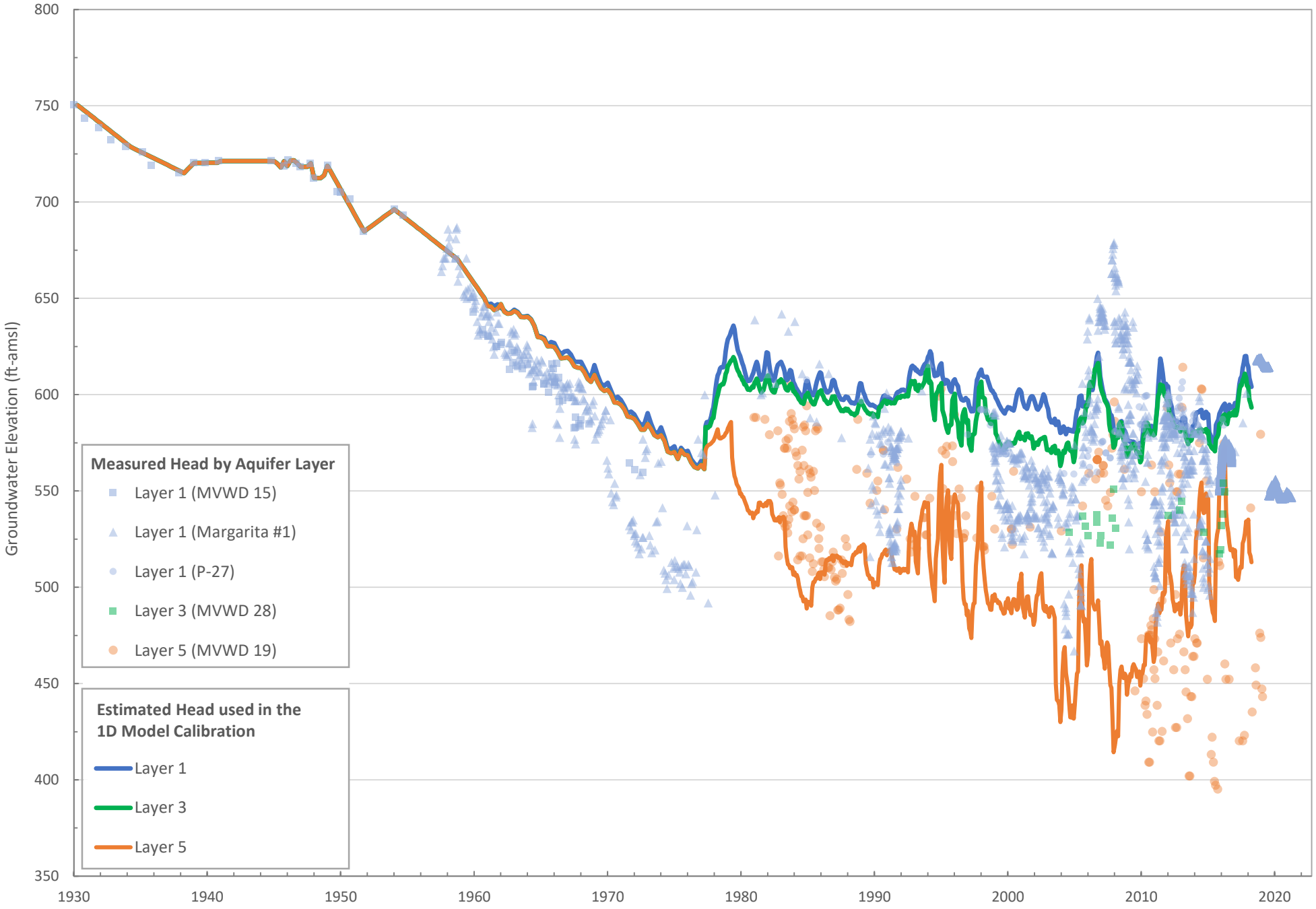

Figure 6. Wells Constructed in Northwest MZ-1 Over Time by Model Layer

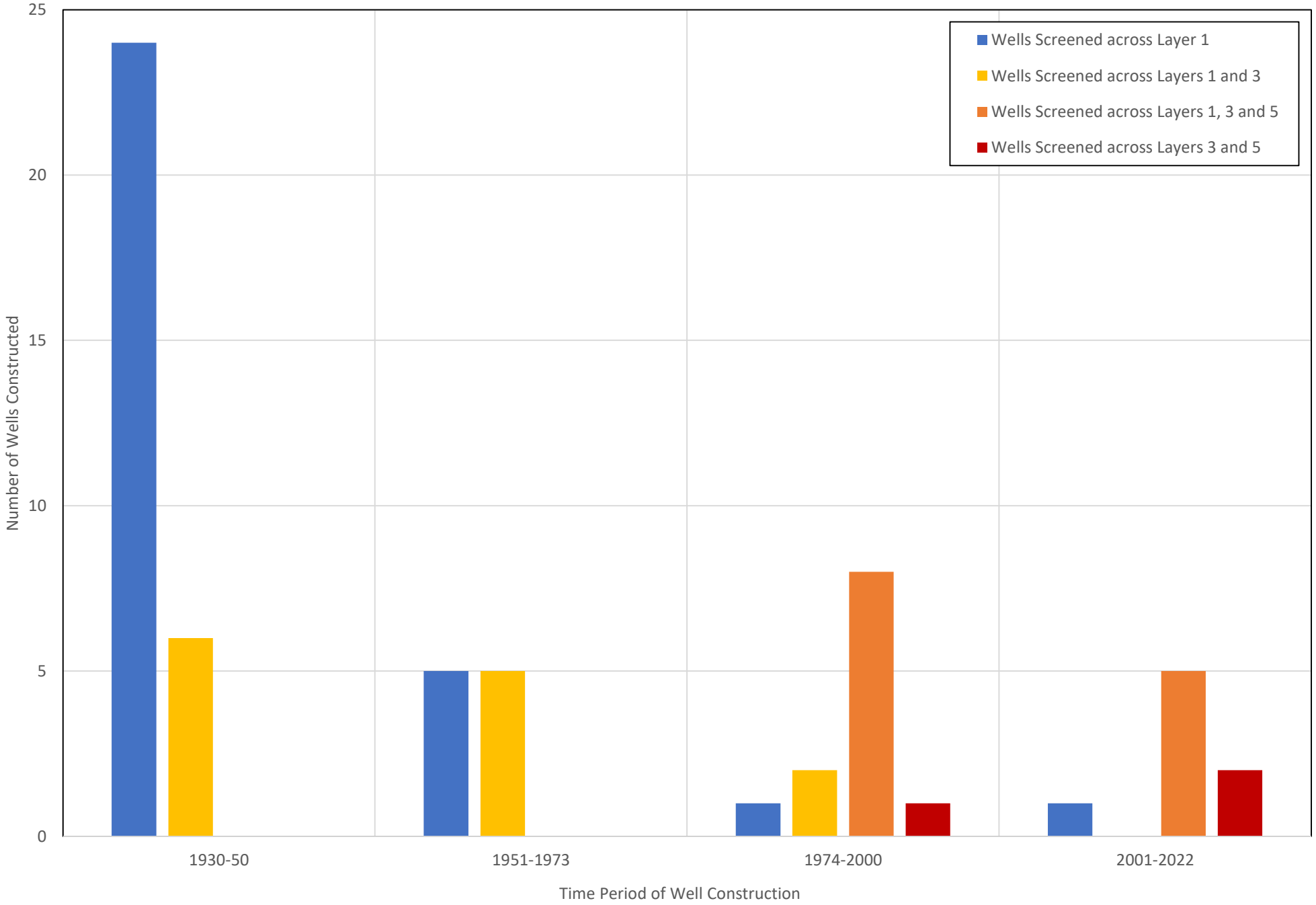

Figure 7. Time Series of the Simulated and Observed Subsidence Values of Selected Calibration Iterations for PX

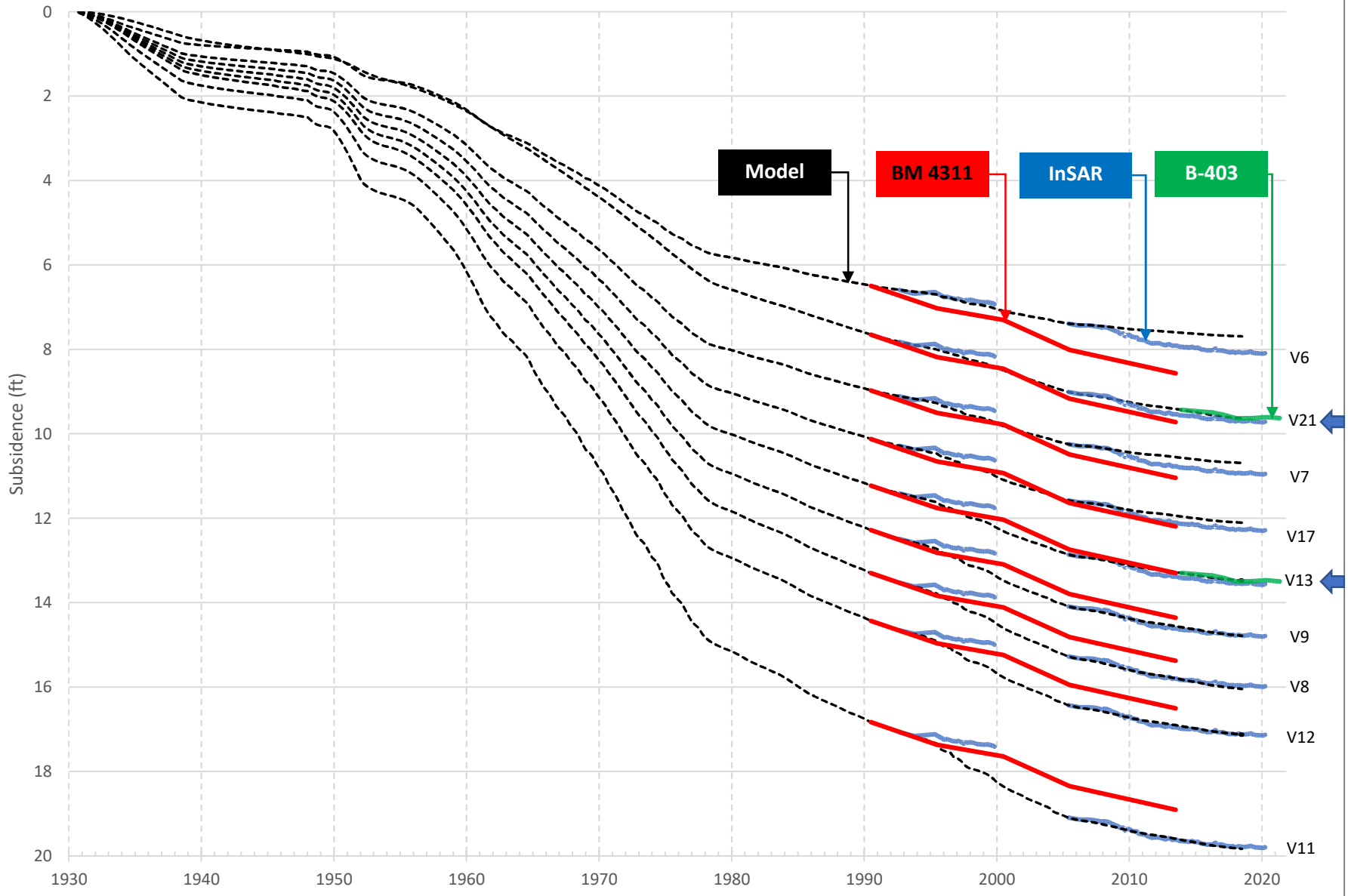

Figure 8. Time Series of the Simulated and Observed Subsidence Values of Selected Calibration Iterations for MVWD-28

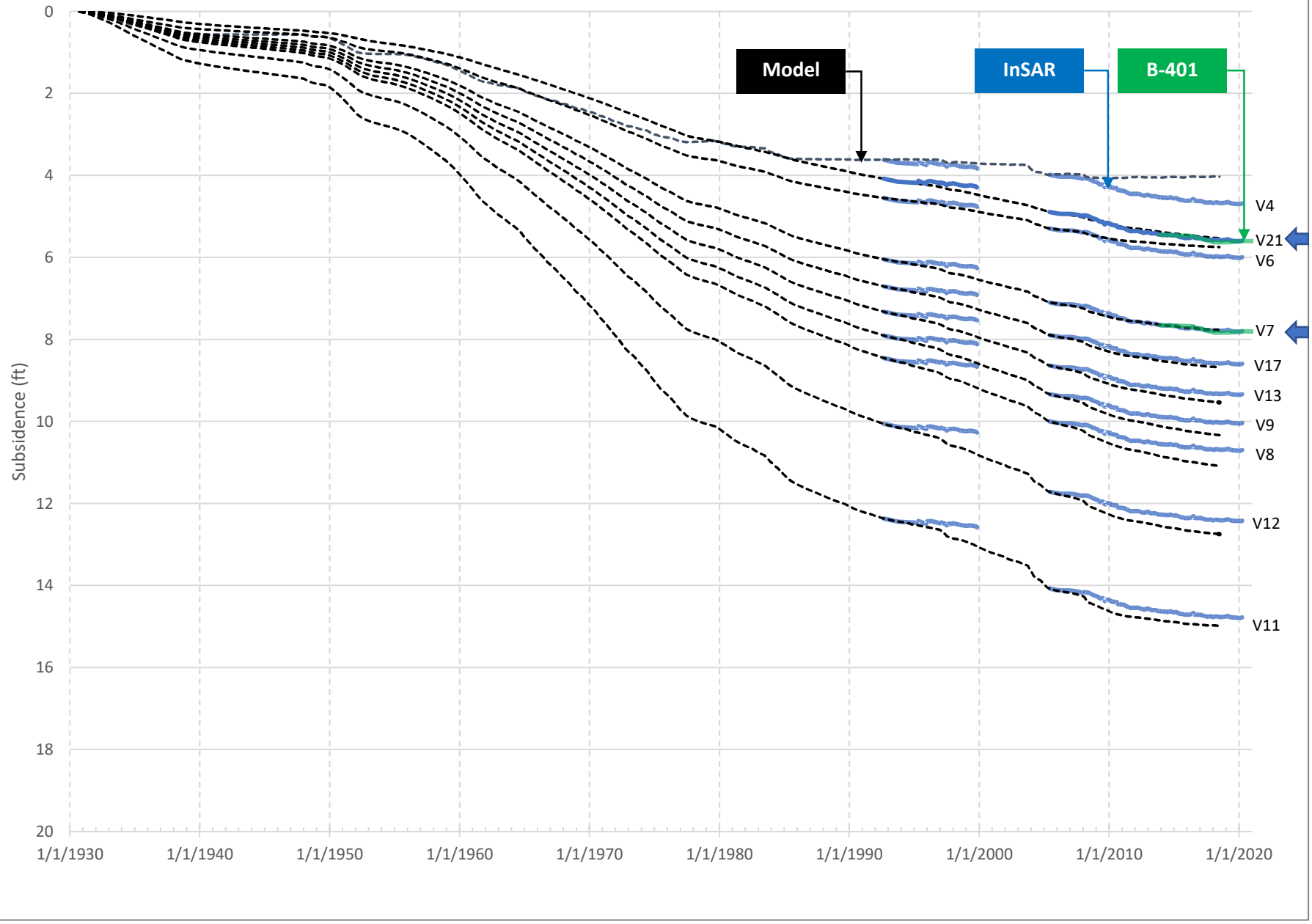

Figure 9. Measured Subsidence vs. Compaction Simulated by PX 1D Model - Calibration Run V21

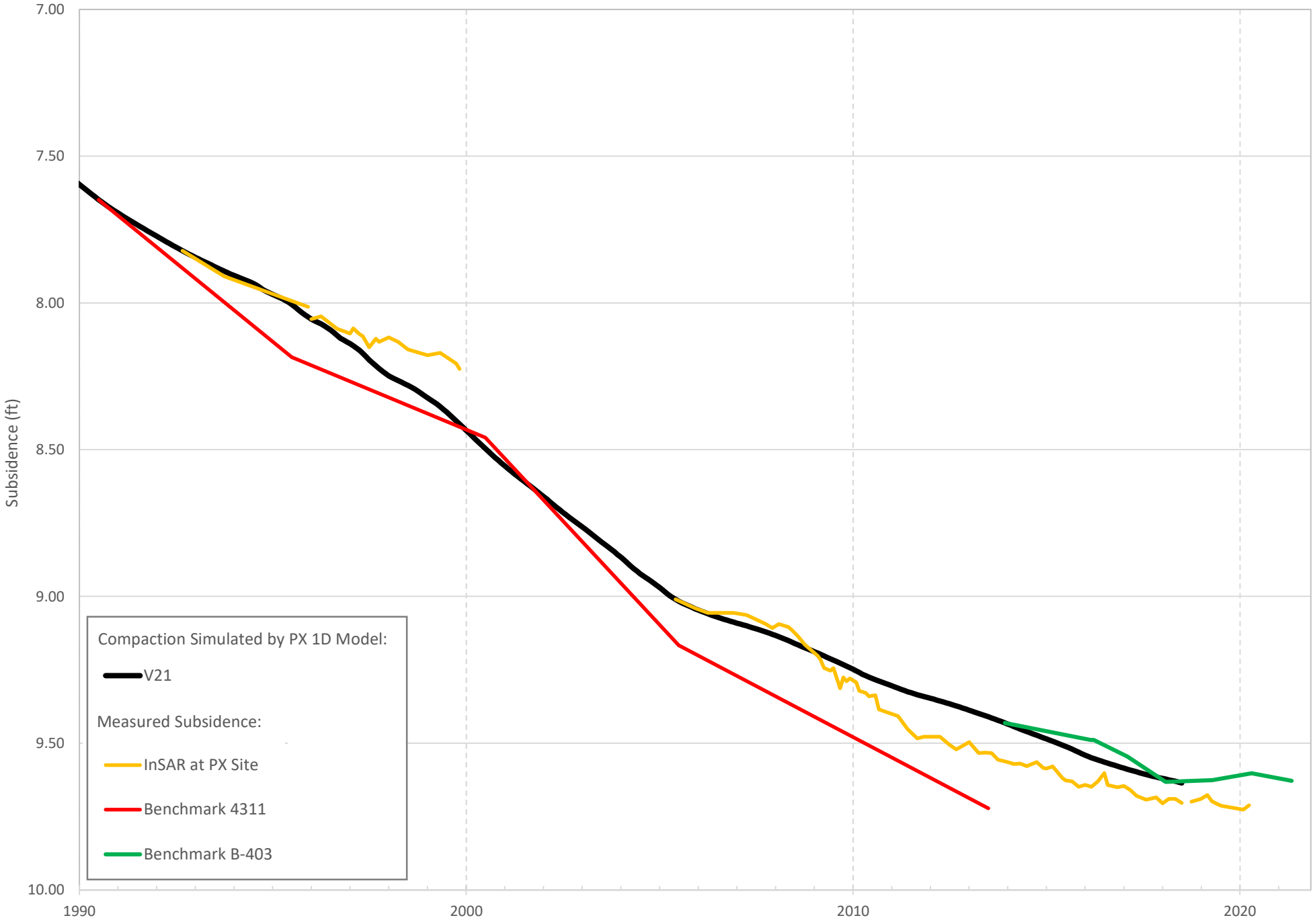

Figure 10. Measured Subsidence vs. Compaction Simulated by MVWD-28 1D Model - Calibration Run V21

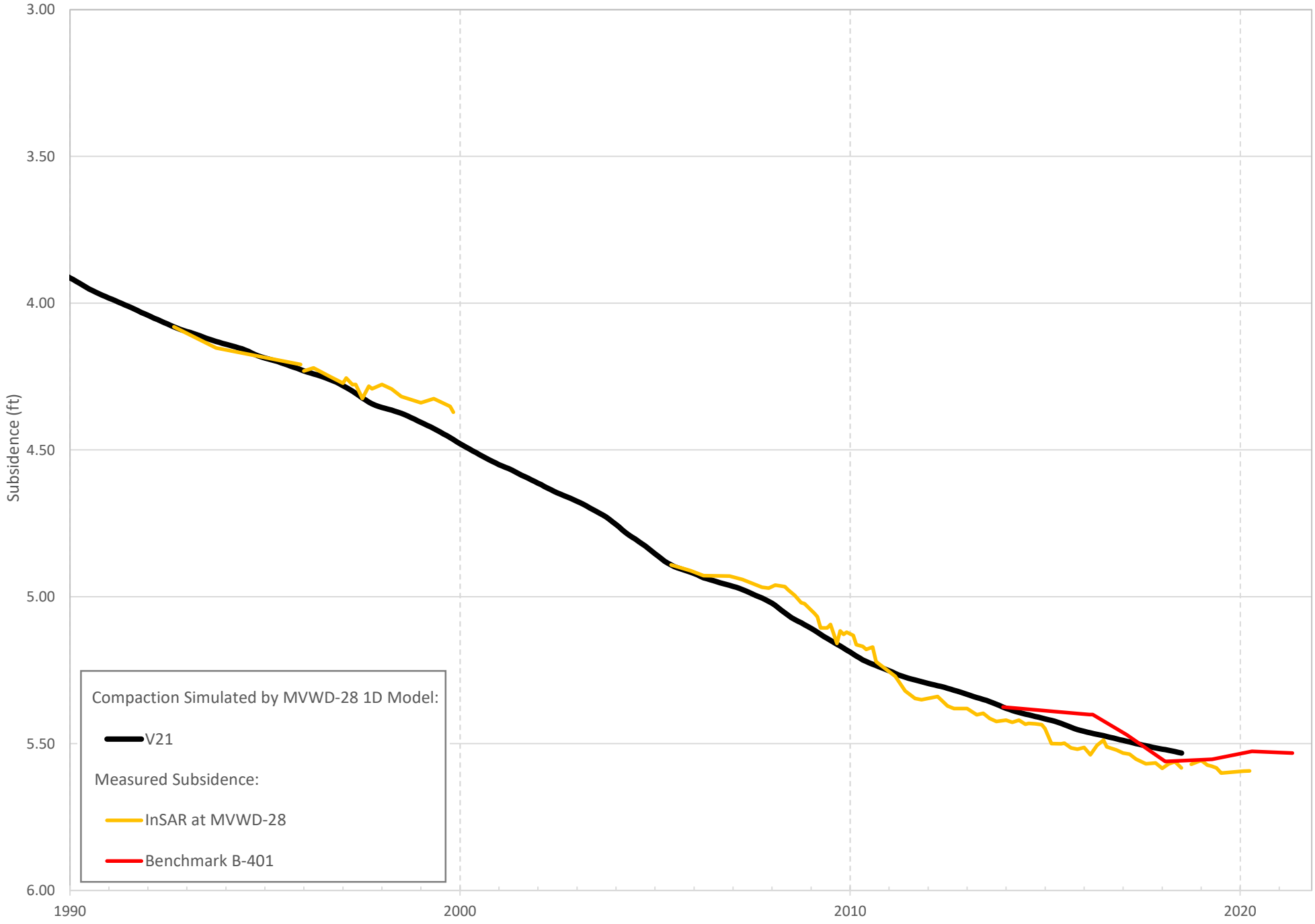

Figure 11. Scatter Plot of the Simulated and Observed Subsidence Values of Calibration Iteration V21 for PX

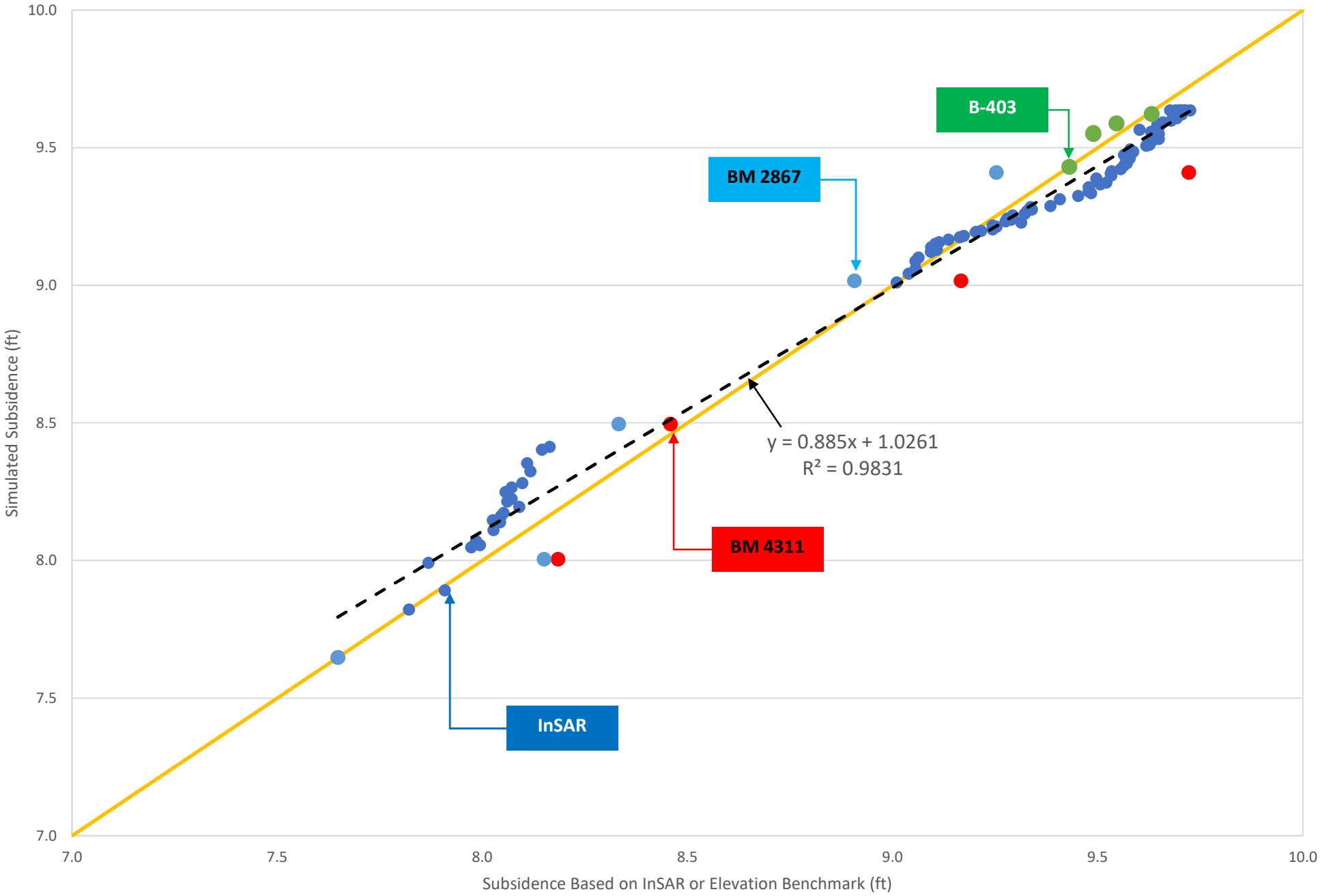

Figure 12. Scatter Plot of the Simulated and Observed Subsidence Values of Calibration Iteration V21 for MVWD-28

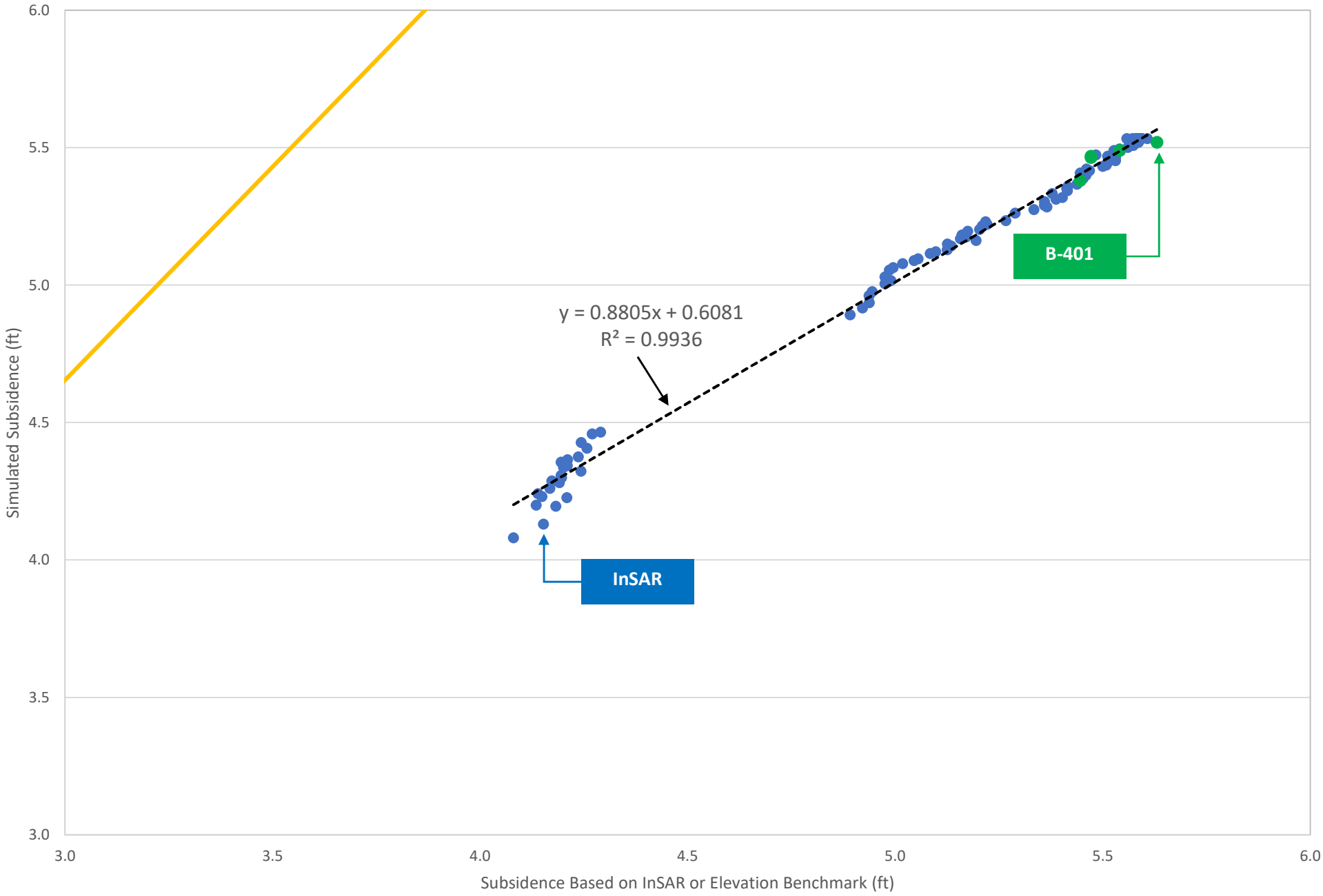

Figure 13. Simulated Compaction and Critical Head on 6/30/2018 for PX

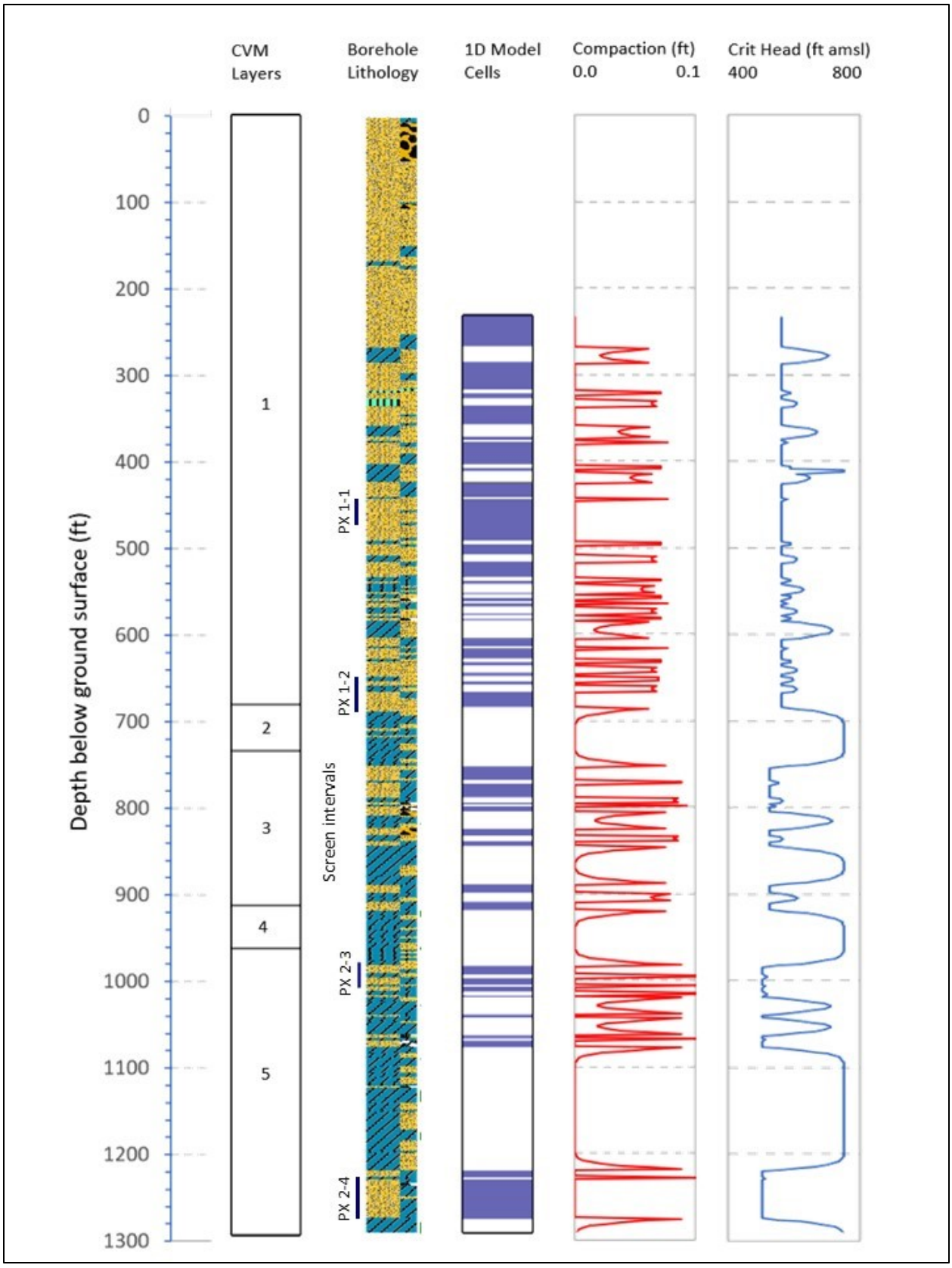

Figure 14. Simulated Compaction and Critical Head on 6/30/2018 for MVWD-28

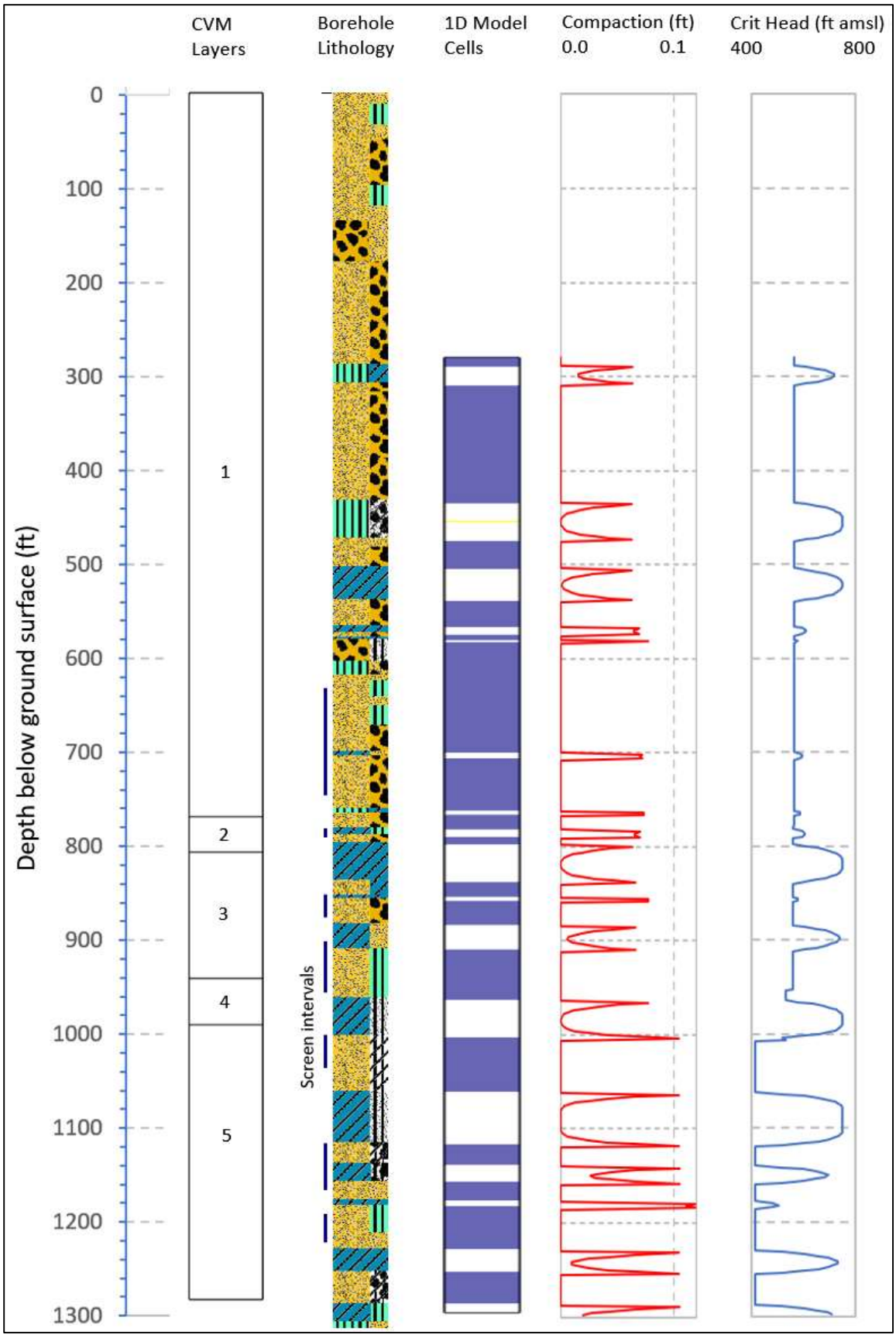

Figure 15. Measured Heads vs. Heads Used in Calibration of PX 1D Model - Calibration Run V22

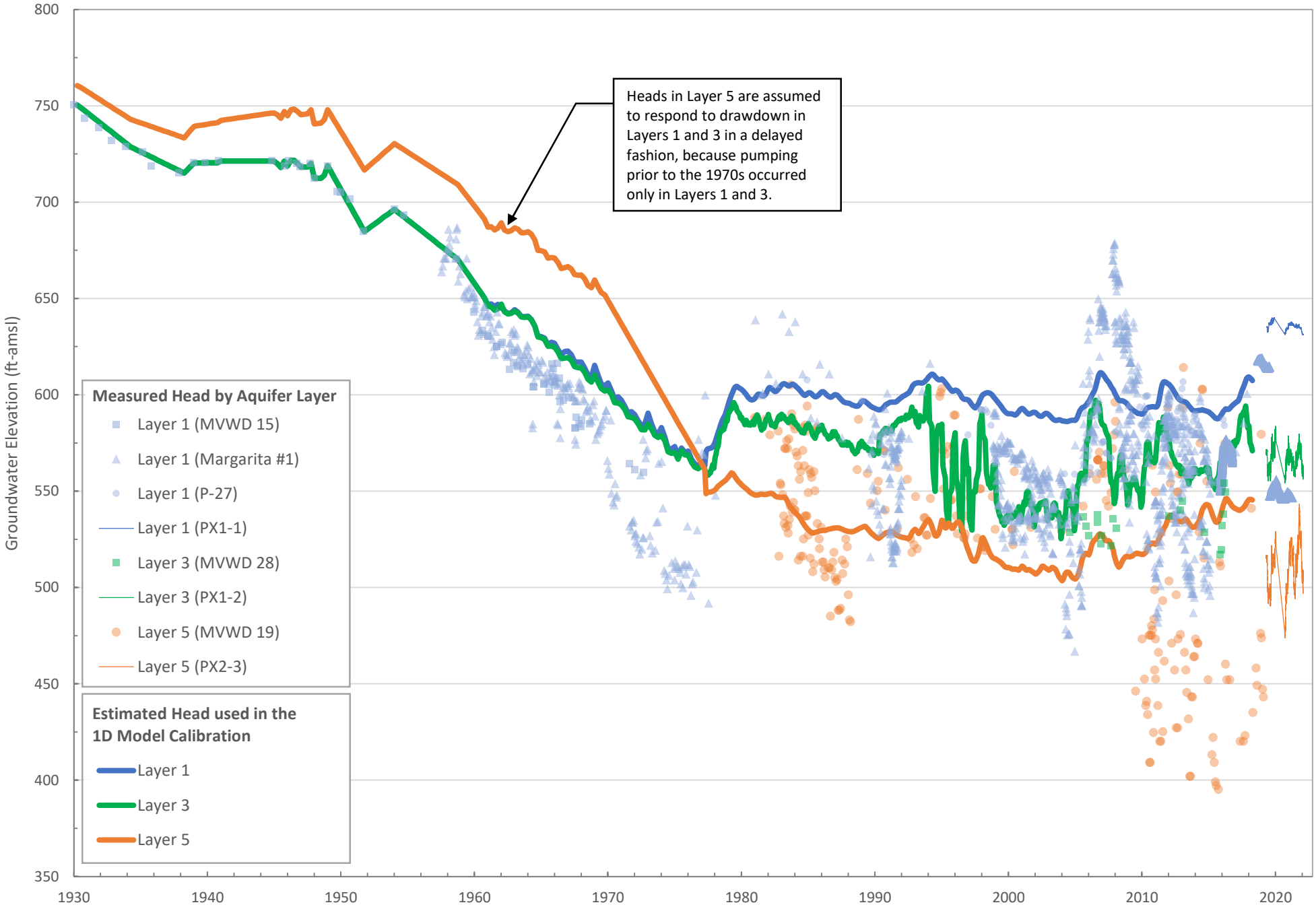

Figure 16. Measured Heads vs. Heads Used in Calibration of PX 1D Model - Calibration Run V23

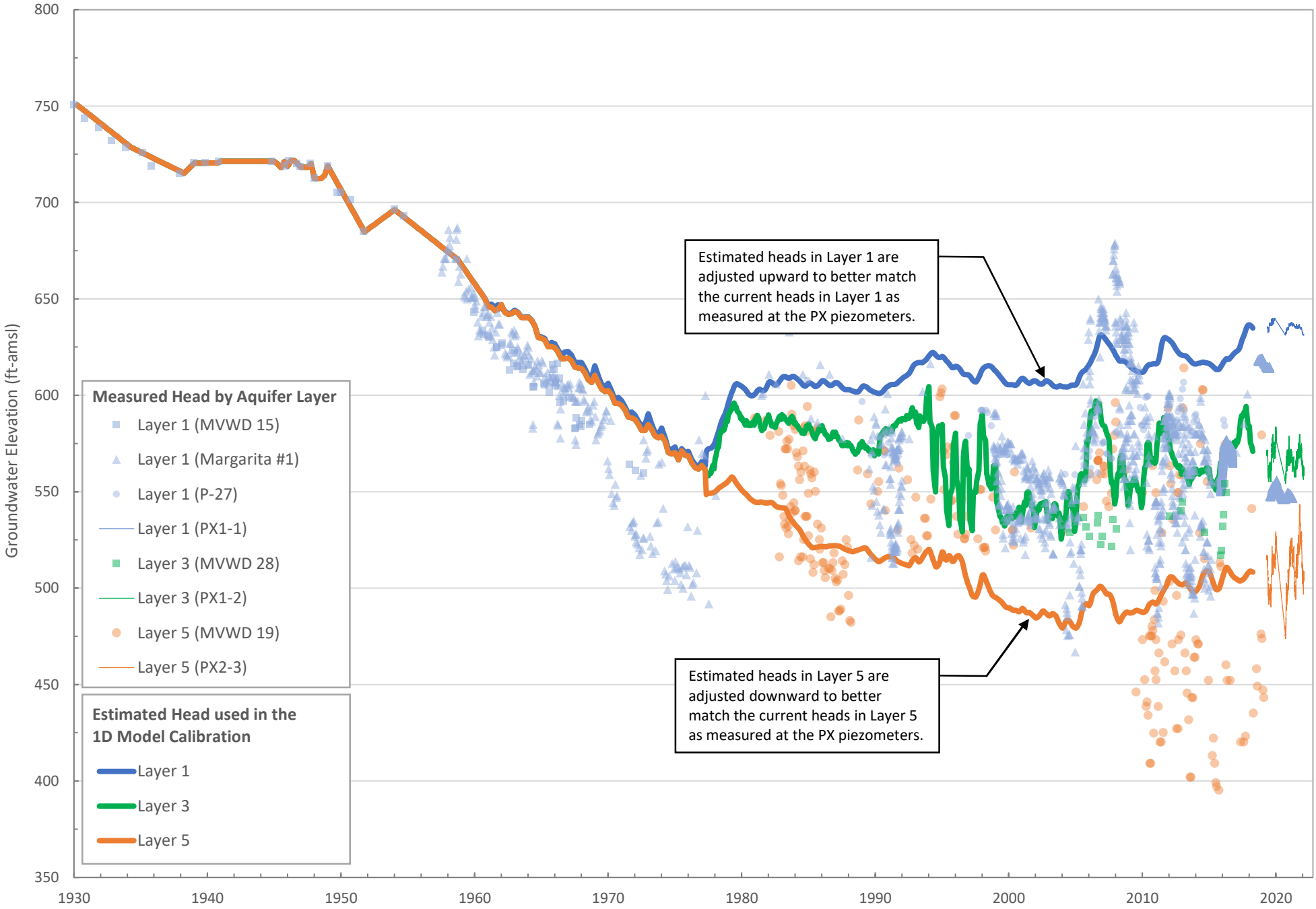

Figure 17. Measured Heads vs. Heads Used in Calibration of PX 1D Model - Calibration Run V24

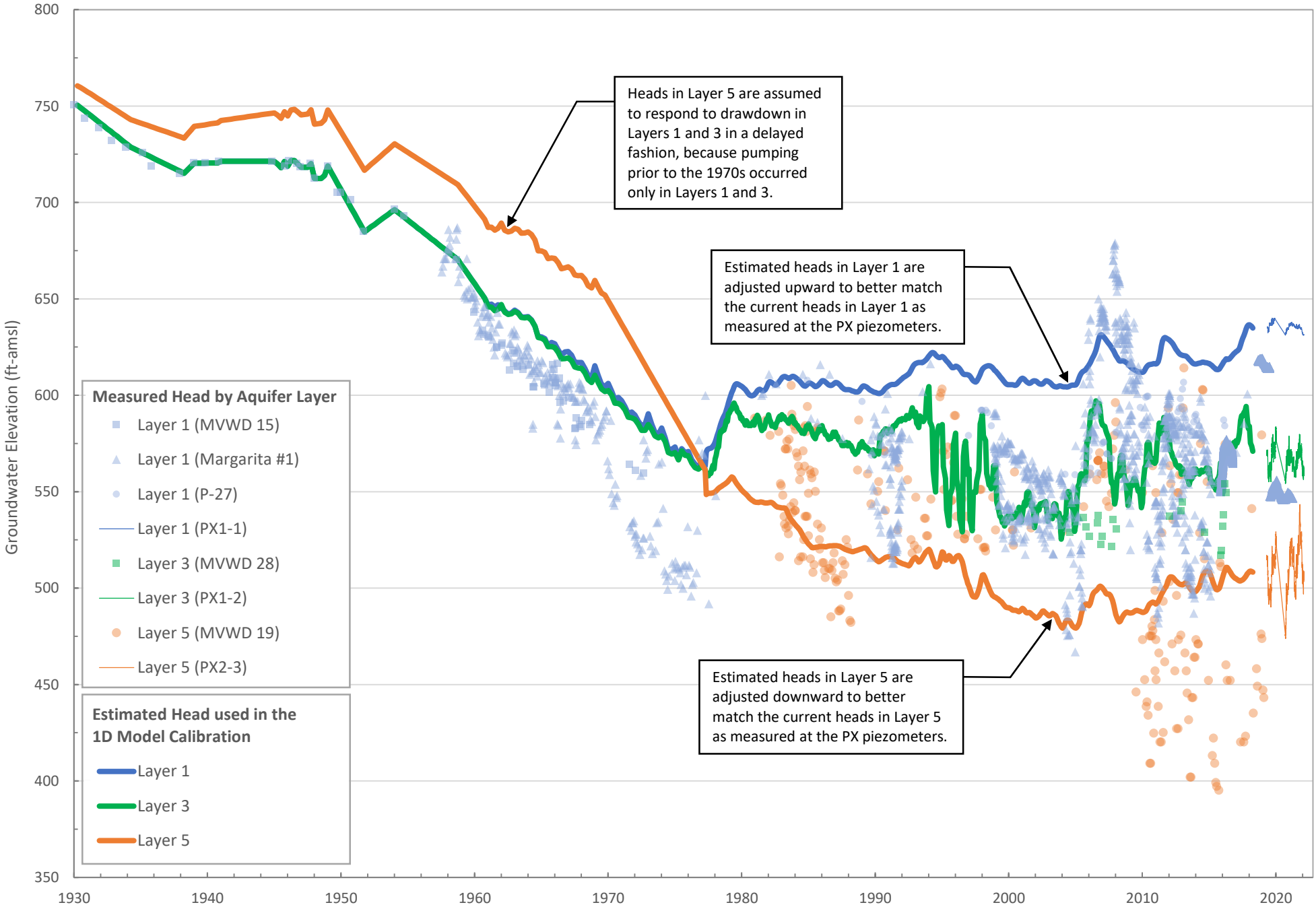

Figure 18. Measured Heads vs. Heads Used in Calibration of MVWD-28 1D Model - Calibration Run V22

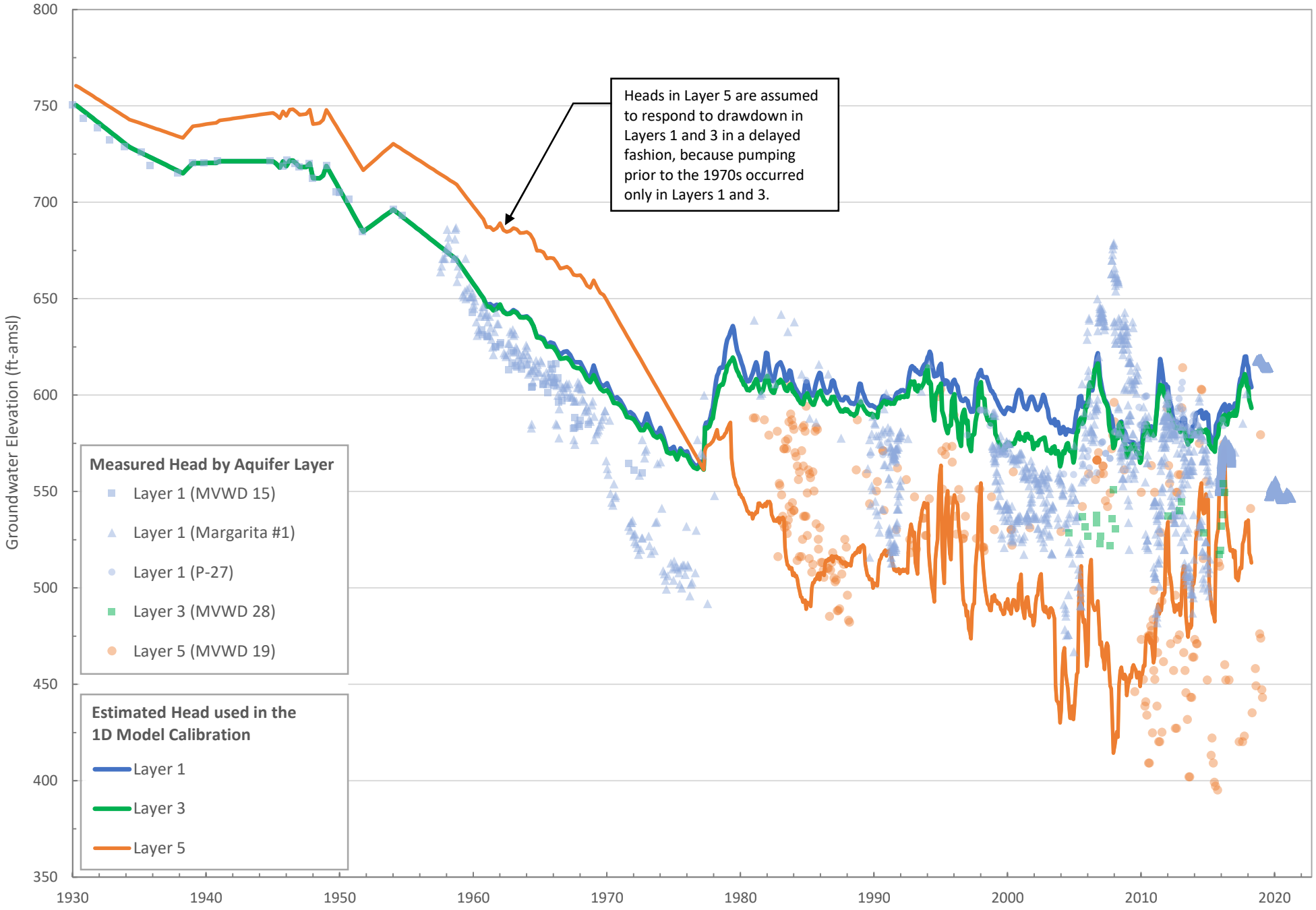

Figure 19. Measured Heads vs. Heads Used in Calibration of MVWD-28 1D Model - Calibration Run V23

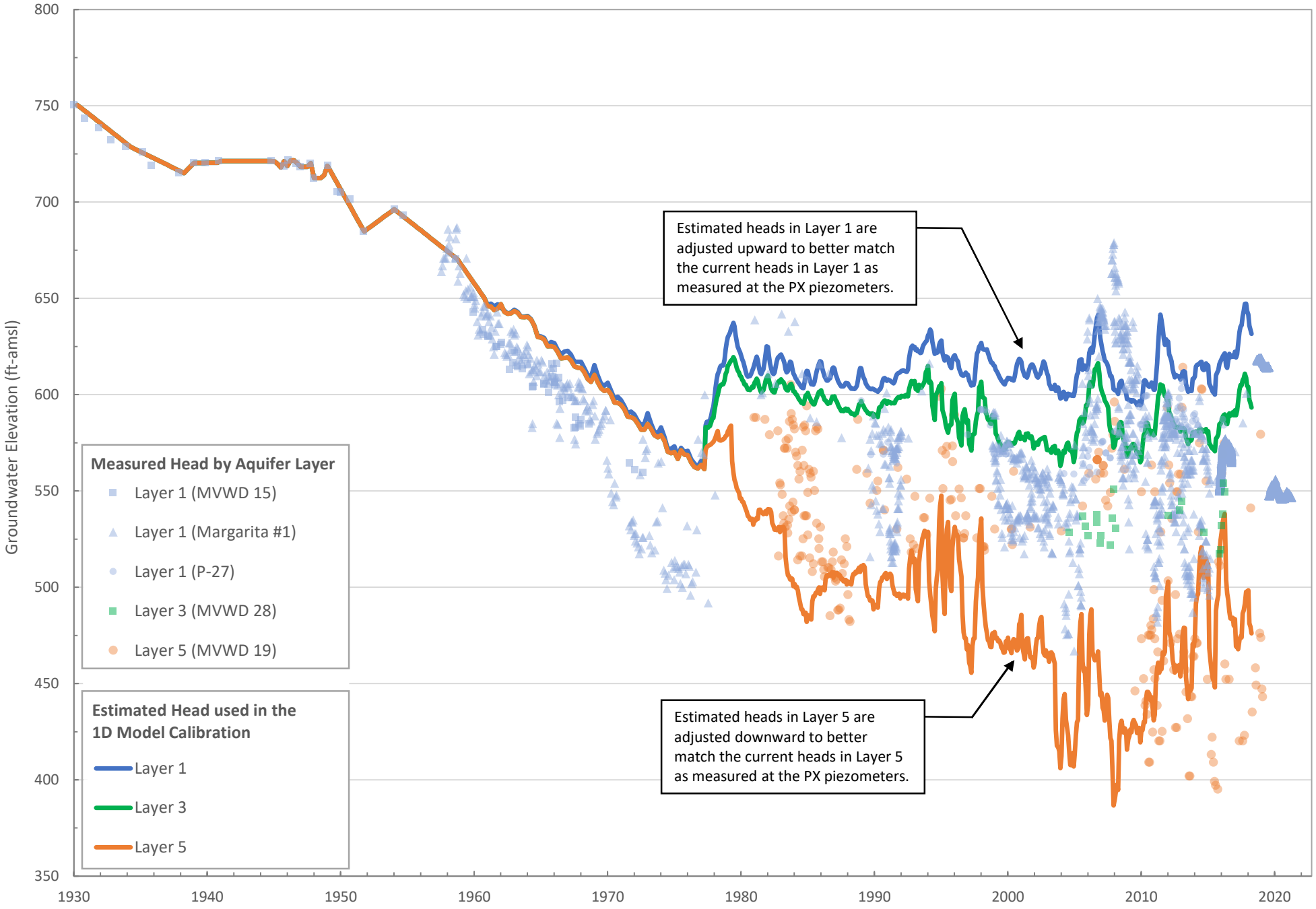

Figure 20. Measured Heads vs. Heads Used in Calibration of MVWD-28 1D Model - Calibration Run V24

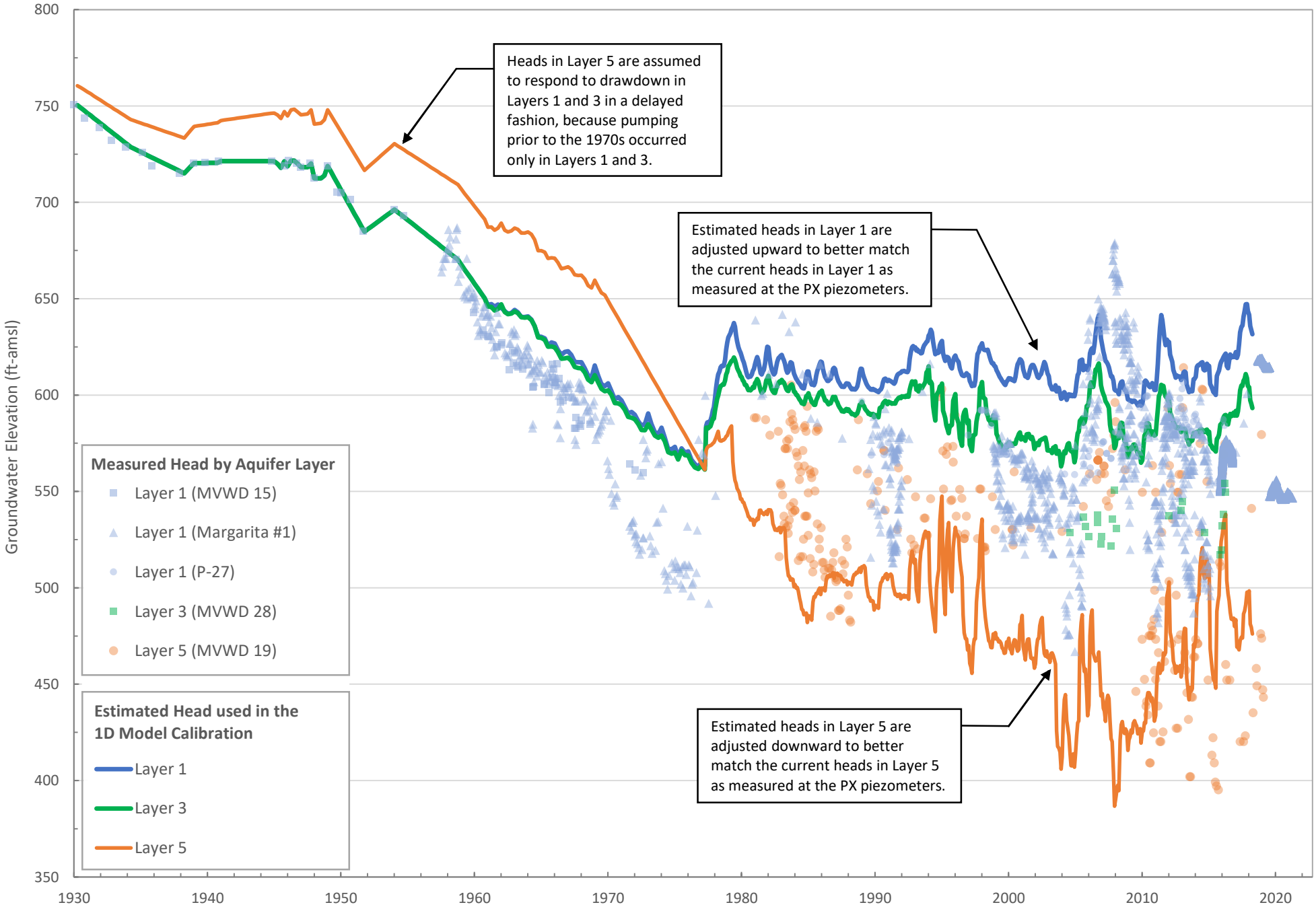

Figure 21. Measured Subsidence vs. Compaction Simulated by PX 1D Model - Calibration Run V22)

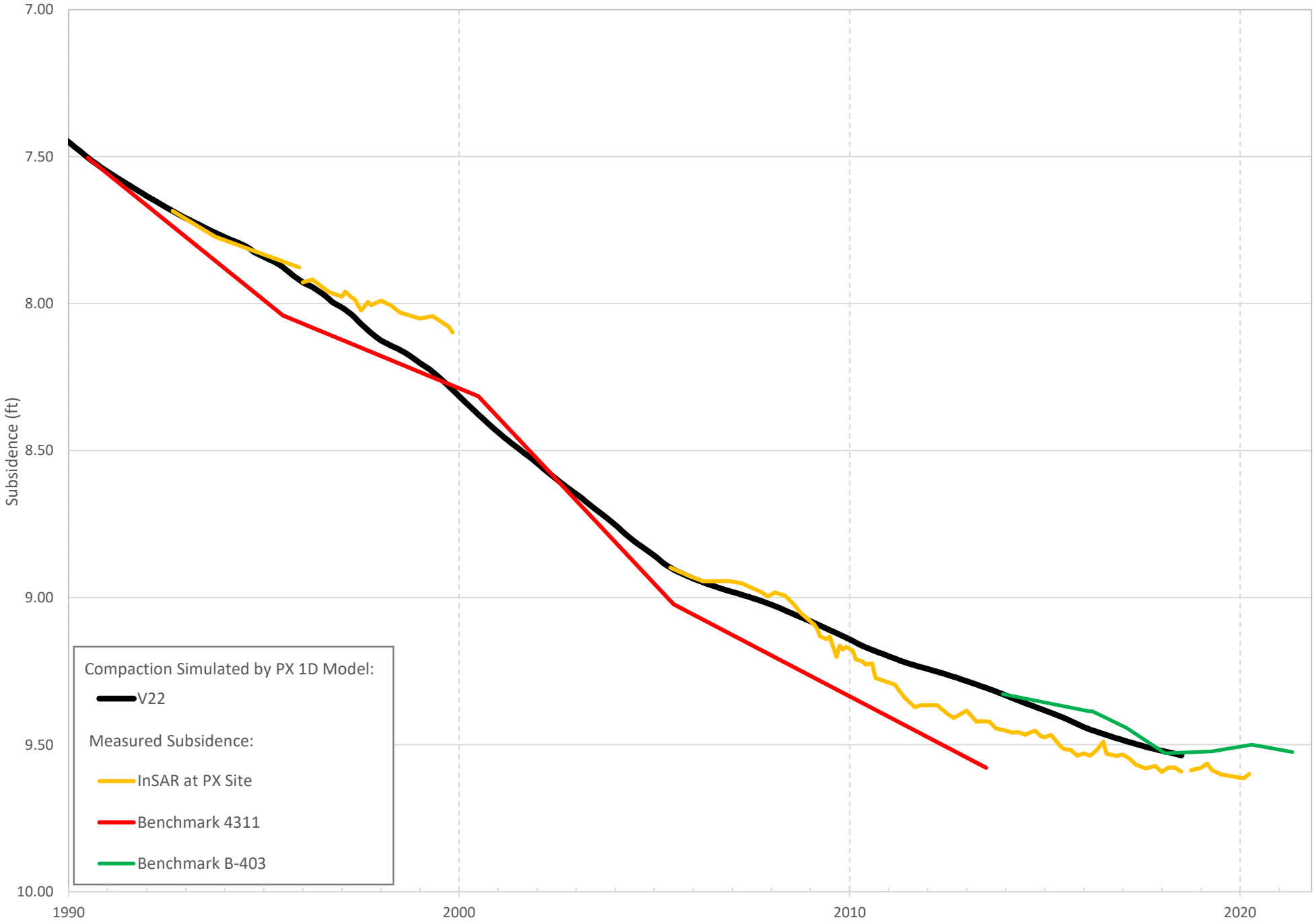

Figure 22. Measured Subsidence vs. Compaction Simulated by PX 1D Model - Calibration Run V23

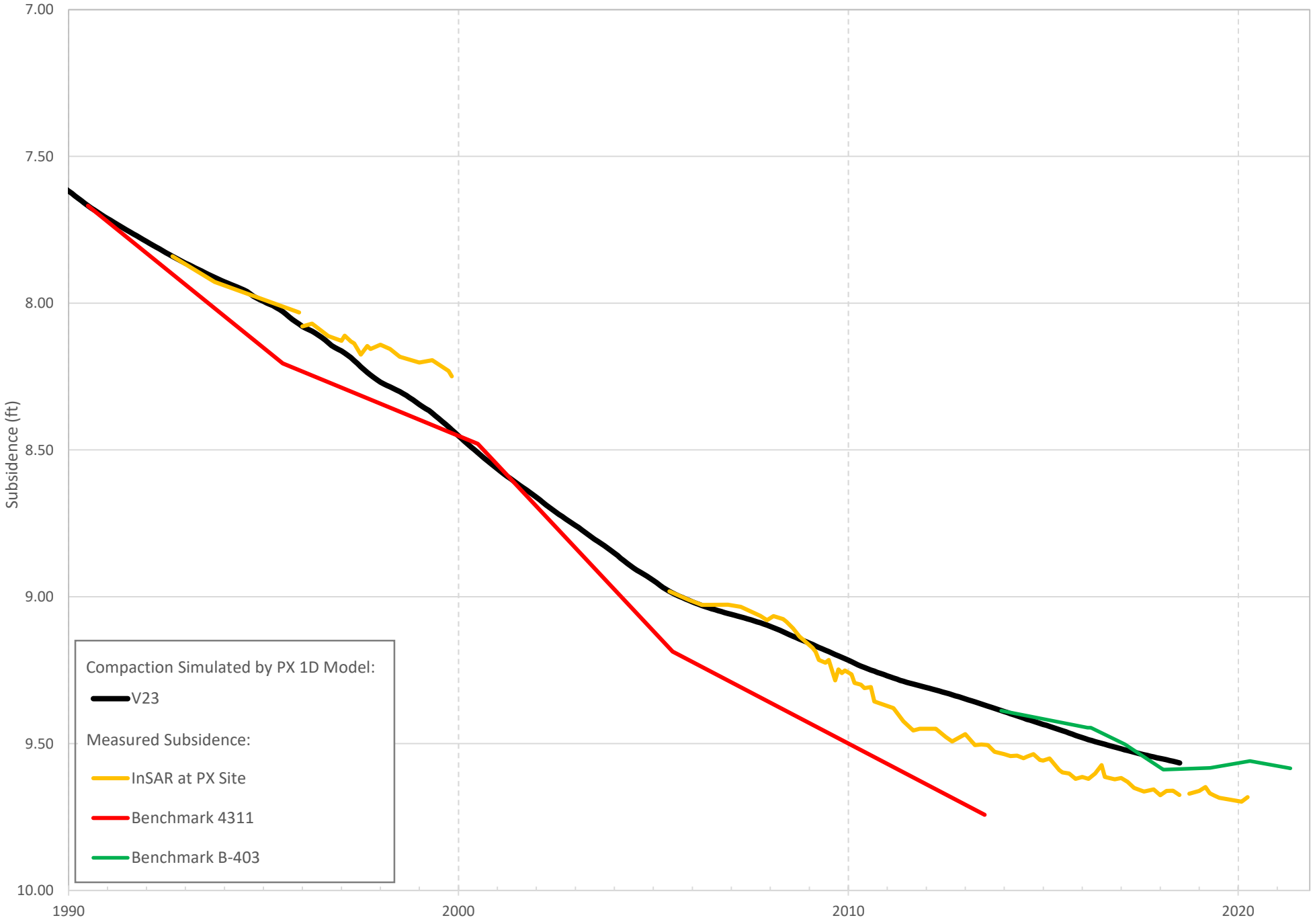

Figure 23. Measured Subsidence vs. Compaction Simulated by PX 1D Model - Calibration Run V24

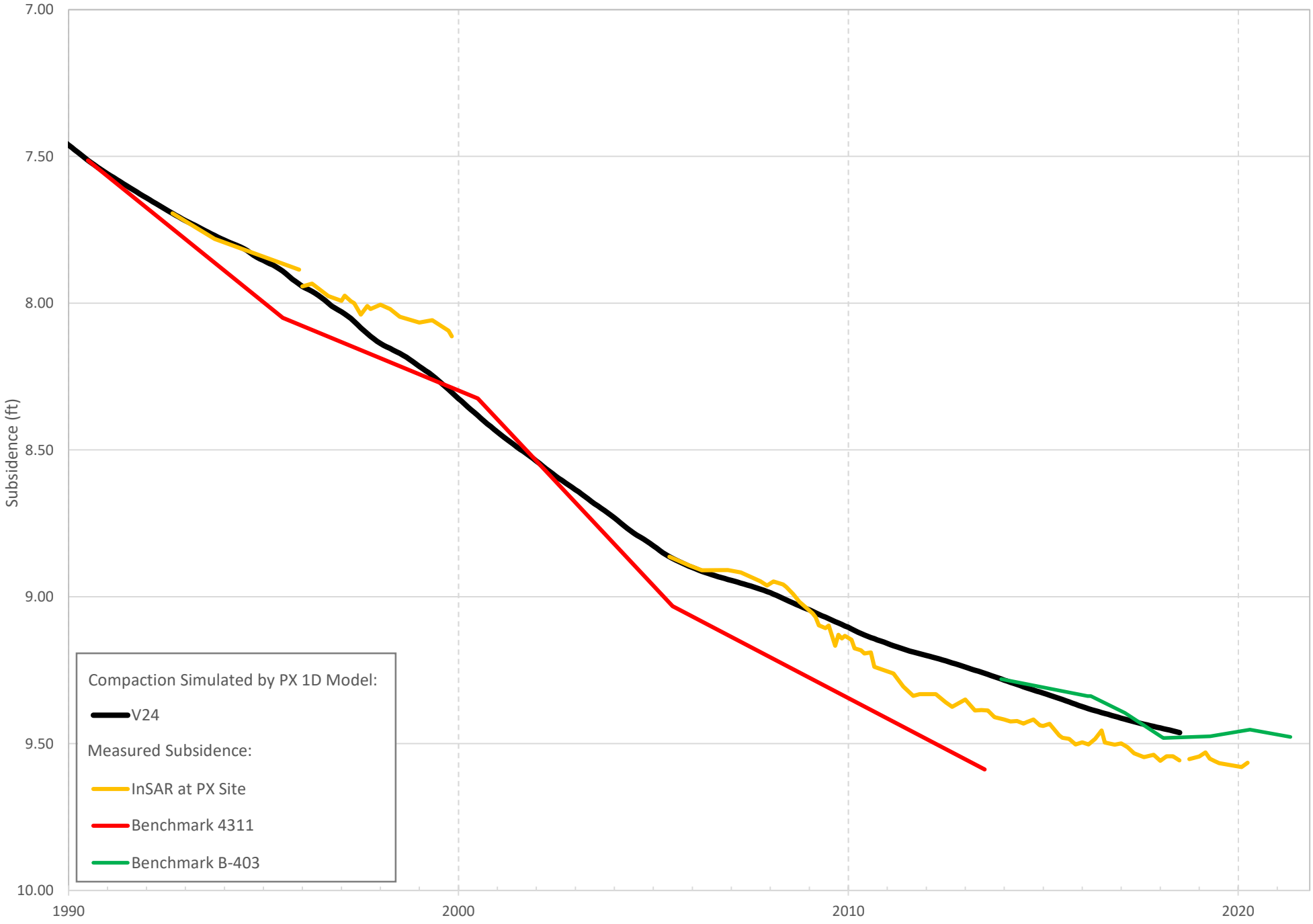

Figure 24. Measured Subsidence vs. Compaction Simulated by MVWD-28 1D Model - Calibration Run V22

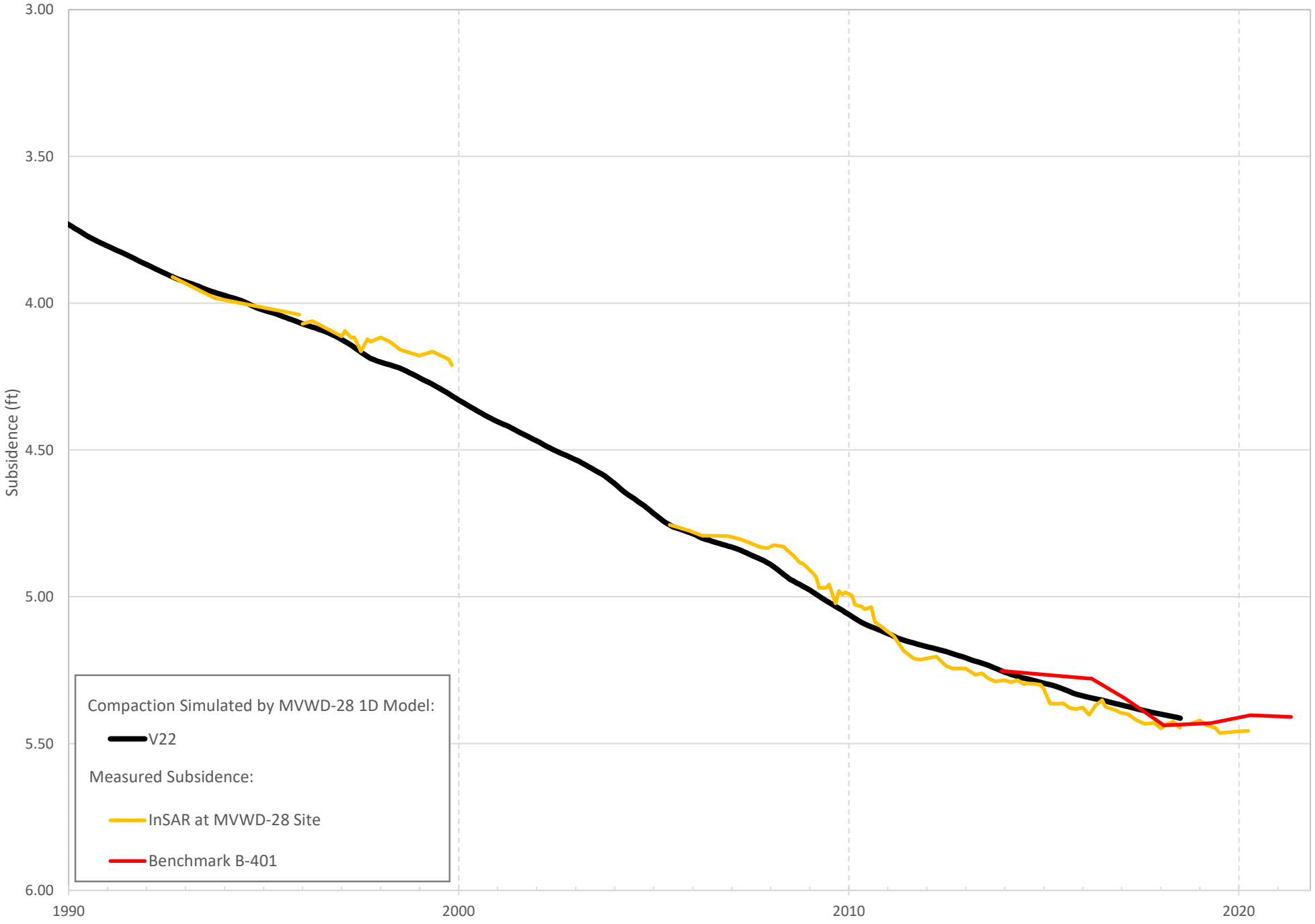

Figure 25. Measured Subsidence vs. Compaction Simulated by MVWD-28 1D Model - Calibration Run V23

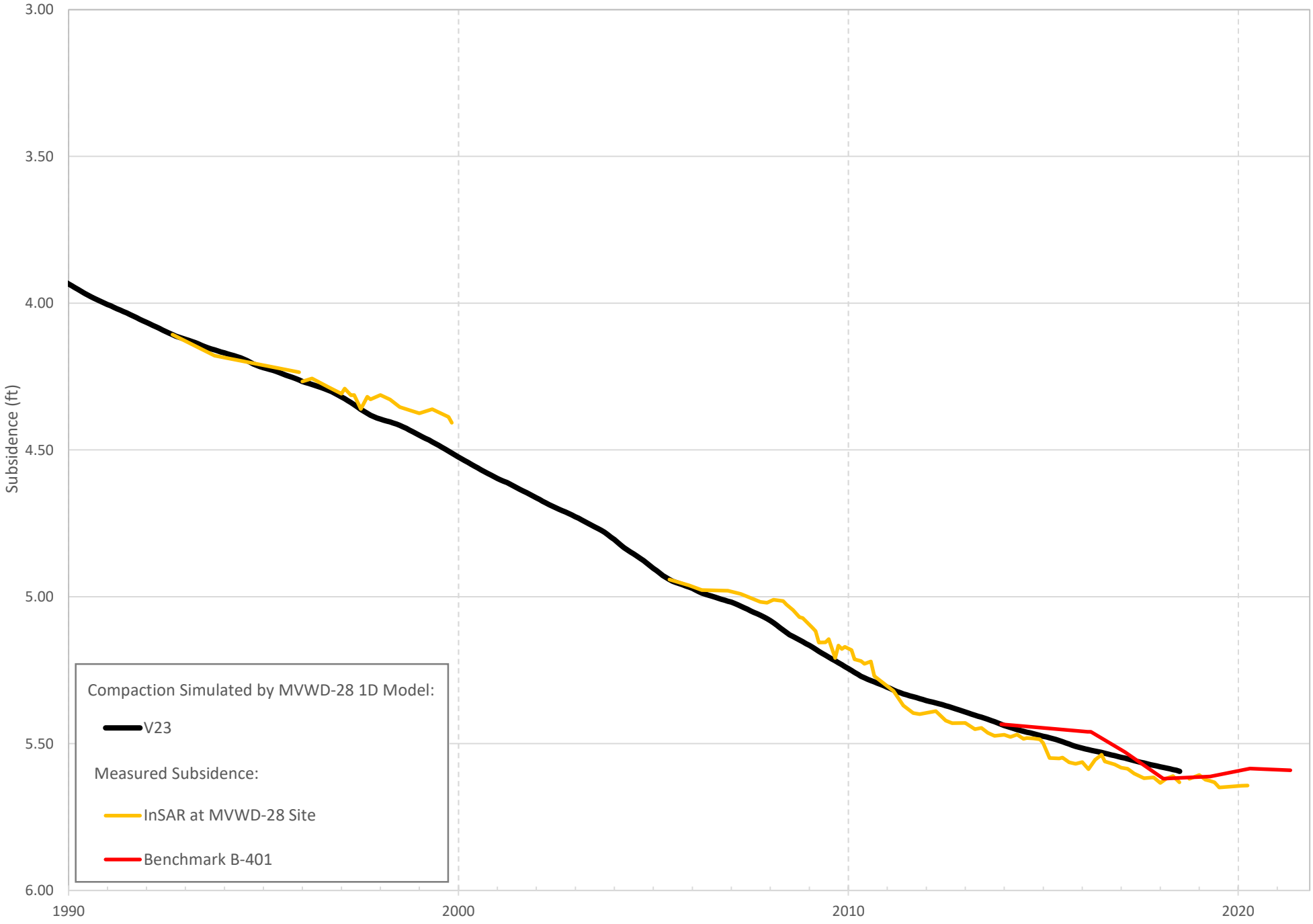

Figure 26. Measured Subsidence vs. Compaction Simulated by MVWD-28 1D Model - Calibration Run V24

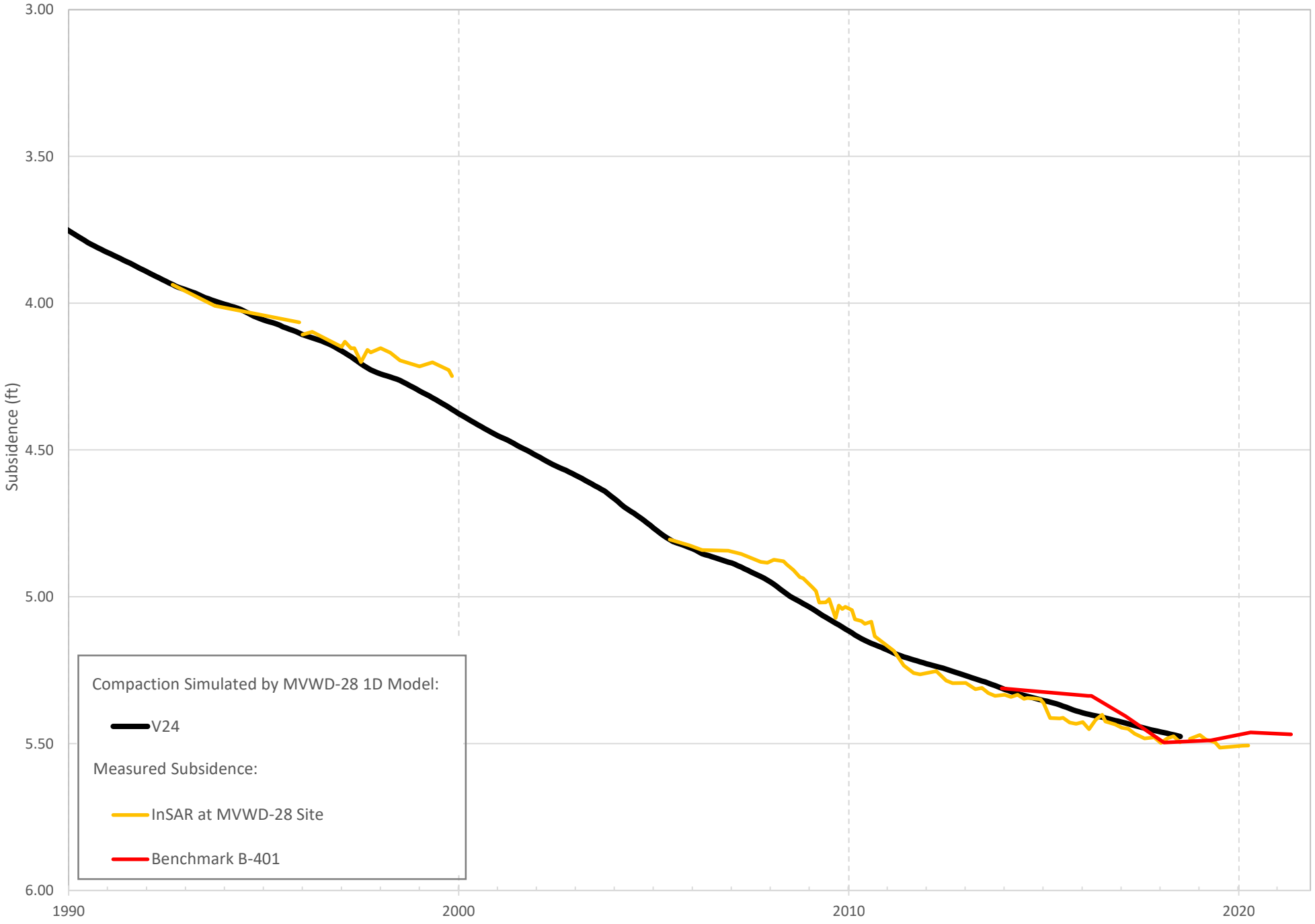

Attachment A

Driller's Logs of PX and MVWD

DRAFT